

# Polymer and metal oxide supported alkali metal naphthalenides: application in the generation of lithium and sodium reagents<sup>1</sup>

Tania R. van den Ancker<sup>a</sup>, Colin L. Raston<sup>b,\*</sup>

<sup>a</sup> Faculty of Science and Technology, Griffith University, Nathan, Qld. 4111, Australia

<sup>b</sup> Department of Chemistry, Monash University, Clayton, Melbourne, Vic. 3168, Australia

Received 26 February 1997

---

## Abstract

Highly coloured paramagnetic polymer supported lithium **5,5'** and sodium **6,6'** naphthalenide complexes have been prepared from the reaction of THF solutions of lithium and sodium biphenylide with polystyrene bearing  $-\text{CH}_2\text{SiMe}_2(\text{C}_{10}\text{H}_7)$  groups. Treating chloropropyl functionalised silica, alumina and titania surfaces with  $\text{H}_3\text{Al} \cdot \text{NMe}_3$  or  $\text{H}_3\text{Ga} \cdot \text{NMe}_3$  afford hydroxyl depleted surfaces. Successive treatment with lithium biphenylide, 1-(chlorodimethylsilyl)naphthalene and an alkali biphenylide affords supported alkali naphthalenide complexes which generate in high yield lithium and sodium reagents when treated with a range of organic halides, nitriles and phosphates, as found for **6,6'** and **7,7'**. © 1998 Elsevier Science S.A.

*Keywords:* Polystyrene; Lithium reagent; Sodium reagent; Silica; Alumina; Titania; Alane; Gallane

---

## 1. Introduction

The use of alkali metal arene radical anion complexes,  $\text{ArH}^{\cdot-} \text{M}^+$ , as soluble sources of metal in the formation of organoalkali metal species from organic halides is well established [1–5] with the early work focusing on the use of lithium naphthalenide [1]. Many radical anion derivatives of lithium have been prepared in recent years which show potential in the synthesis of alkyllithium reagents. Lithium 4,4'-di-*t*-butylbiphenyl (LiDBB) [6] is particularly noteworthy in that while it acts as a source of lithium, removal of the DBB by-product is facilitated by its low volatility [3].

Another approach to overcoming the objection of having solutions of the target organoalkali metal species loaded with the arene by-product is the use of a catalytic amount of the arene [7,8]. Here, the arene undergoes electron transfer with bulk metal affording a radical anion complex which then reacts with RX with regeneration of the arene to complete the catalytic cycle. Various percentages (1–20%) and types of arene

have been studied, including naphthalene, biphenyl and 4,4'-di-*t*-butylbiphenyl. In these reactions only small amounts of the by-product arene is present in the product mixtures. Chromatography is still required, however, when pure compounds are needed. In this way, reactions of several types of organic chlorides have been investigated including chloroketals [9], aryl chlorides [10], dichlorobutenes [11] and chloromethyl ethyl ether [12]. The same approach has also been used in the preparation of lithium complexes from trialkylphosphates [13], nitrile complexes [14] alkyl phenyl sulfones [15], dialkyl sulfates [16], and phenyl sulfides [15]. Such reactions are usually carried out, under argon at low temperatures at ca.  $-78^\circ\text{C}$  in a coordinating solvent, whereby a solution of the organic reagent in THF for example is added to a suspension of lithium in the same solvent, to which a catalytic amount of arene has been added. The mixture is then stirred for 0.5–12 h prior to quenching with an electrophile. For reactions that are of a Barbier-type, the electrophile is added to a lithium arene slurry before addition of RX.

A variety of new lithium complexes have been prepared using arene catalysed reaction of organochlorides with lithium, for example 2-(3-lithiopropyl)-1,3-dioxolane which offers a direct synthesis to  $\gamma$ -lactones when treated with carbonyl compounds [17]. Similarly,

---

\* Corresponding author.

<sup>1</sup> Dedicated to Professor Ken Wade on the occasion of his 65th Birthday in recognition of his outstanding contribution to organometallic and inorganic chemistry.

a variety of alcohols, dienic alcohols, and cyanoxepanes have been isolated from reactions of masked lithium  $\delta$ -enolates [18].

Another approach to overcome generating solutions of organoalkali metal species loaded with arene is the use of supported radical anion species. This is the theme of the work described herein which investigates the preparation of supported alkali metal naphthalenide complexes and their utility in forming lithium and sodium reagents. It is an extension of a preliminary account of the synthesis of polymer supported alkali metal naphthalenides and their reactivity with organic complexes [1] and of our studies on polymer [19,20] and silica [21] supported magnesium anthracene complexes which afford arene free solutions of Grignard reagents in high yield when treated with benzylic halides.

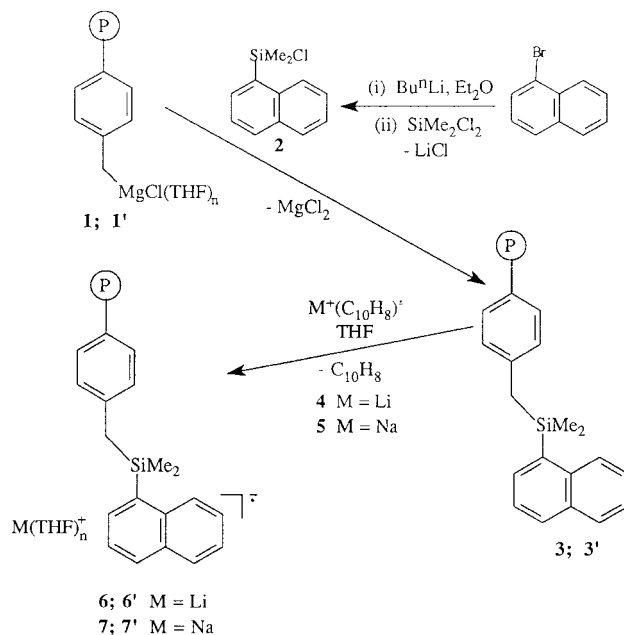
## 2. Results and discussion

### 2.1. Polymer supported alkali metal naphthalenides

Treatment of a THF slurry of the Grignard reagent of ca. 1% crosslinked chloromethylated polystyrene **1,1'** (1.20–1.34 and 4.11–4.15 mmol g<sup>-1</sup> Cl, respectively) with excess 1-(chlorodimethylsilyl)naphthalene, **2**, yielded the naphthalene functionalised polymer **3,3'**, Scheme 1, in greater than 95% yield based on weight increase, IR studies and analysis for residual chlorine content. Compound **2** was prepared by quenching 1-lithionaphthalene with excess dichlorodimethylsilane [22].

Reactions involving modification of the chloromethylated polystyrene were monitored by (i) changes in  $\nu_{C-H}$  bending mode of the methylene group [23], displaced from 1265 cm<sup>-1</sup> to 1254 cm<sup>-1</sup> on converting the chloride to the silane, and (ii) the appearance of characteristic absorption bands at 1253 and 847 cm<sup>-1</sup> (shoulder), assigned to Si–C stretching and Si–Me deformations, respectively [23].

Lithium biphenylide **4** and sodium biphenylide **5** were chosen as the electron transfer reagents because of their low reduction potential (–2.70 V vs. SCE) relative to that of lithium naphthalenide (2.50 V vs. SCE), thus in principle facilitating transfer from the biphenyl to naphthalene respectively [24]. Solutions of lithium biphenylide in THF were added to THF slurries of polymers **3,3'** resulting in the formation of red-brown paramagnetic mixtures ( $g_{av} = 2.0034, 2.0035$ ) of polymer supported lithium naphthalenide **6,6'**. Similarly, addition of a THF solution of sodium biphenylide to THF slurries of polymers **3,3'** resulted in the formation of red-brown paramagnetic solutions ( $g_{av} = 2.0034, 2.0035$ ) of polymer supported sodium naphthalenide **7,7'**.



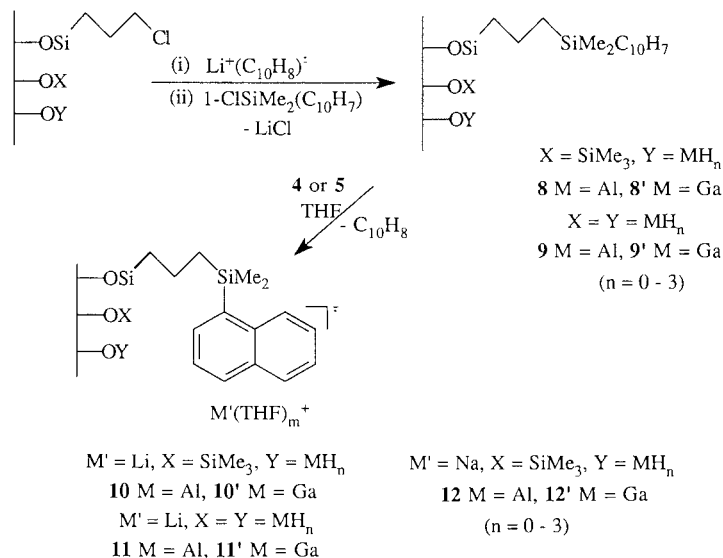
Scheme 1.

### 2.2. Metal oxide supported alkali metal naphthalenides

Reactions of 'endcapped' lithiopropyl silica (prepared via reaction of 'endcapped' chloropropyl silica and lithium biphenylide [21]) with the chlorosilane **2** afforded the silica supported naphthalene complexes as pale cream powders **8, 9** (**8'**, **9'**). Subsequent reactions with the corresponding metal biphenylide afforded the lithium **10, 11** (**10'**, **11'**) or sodium **12** (**12'**) silica supported silylnaphthalenide complexes, Scheme 2. Loading of the naphthalene functionality was determined by the quantity of isolated LiCl by-product. Analysis of silica supports **8, 9** showed the level of loading was 0.85 mmol g<sup>-1</sup> and 1.19 mmol g<sup>-1</sup>, respectively.

Silica supported aminonaphthalene **13** was prepared by refluxing a mixture of silica, *N*-methyl(amino)propyltrimethoxysilane, 1-chloromethylnaphthalene and triethylamine in a toluene/methanol mixture. 'Endcapping' was achieved by treating **13** with chlorotrimethylsilane and/or H<sub>3</sub>Al·NMe<sub>3</sub>, **14, 15** (or H<sub>3</sub>Ga·NMe<sub>3</sub>, **14', 15'**). Subsequent reactions with the corresponding metal biphenylide afforded lithium **16, 17** (**16'**, **17'**) or sodium **18, 19** (**18'**, **19'**) silica supported aminonaphthalenide complexes, Scheme 3. Alumina and titania supported aminonaphthalenide complexes were prepared by methods similar to the silica supported material, albeit with significantly lower loading levels, 0.38 and 0.19 mmol g<sup>-1</sup>, respectively.

For both the silyl and aminonaphthalene metal oxide complexes uptake of the alkali metal depended on the choice of 'endcapping'. For metal oxide complexes that



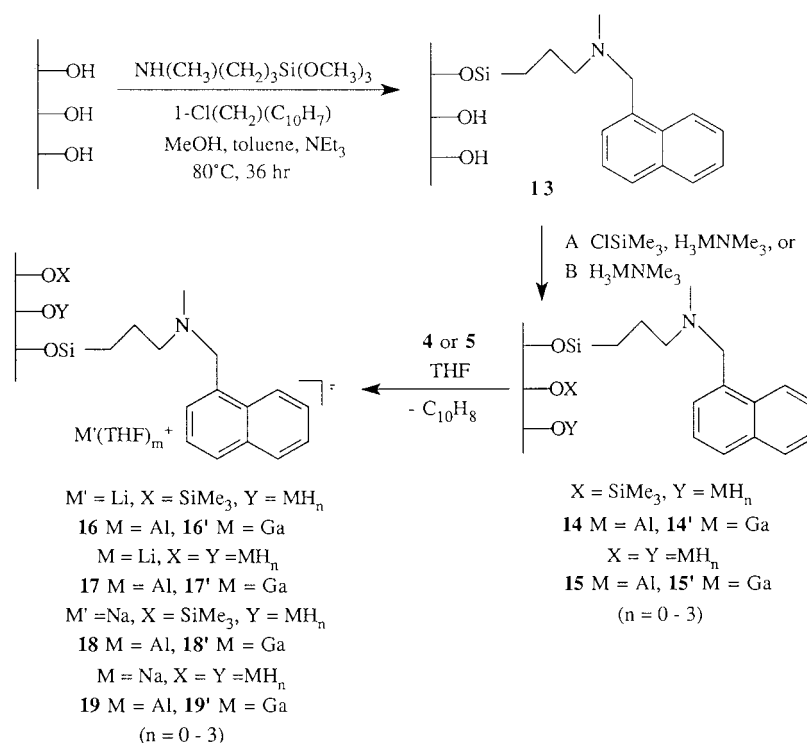
Scheme 2.

were only 'endcapped' with trimethylsilyl groups, a several fold excess of the corresponding biphenylide was required to generate the metal complex, only then in very low yield. Thus, these complexes are unsuitable as reagents for generating organolithium/sodium complexes. In contrast, metal oxides 'endcapped' with aluminium hydride, or a mixture of aluminium hydride/trimethylsilyl groups reacted with the corresponding biphenylide readily, generating the target metal

arene complexes in approximately 75% yield, and these were found to be suitable reagents for the generation of organo alkali complexes on reaction with RX.

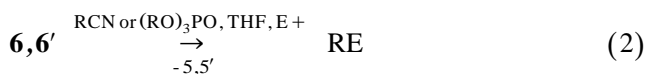
### 2.3. Preparation of lithium reagents

Reactions of the organoalkali complexes were based on two different methods [1–5]. The first involved the formation of the organoalkali, which was then quenched



Scheme 3.

to give the target complex, Eq. (1). The second reaction involved the quenching of the organoalkali complex in situ, a Barbier-type reaction, Eq. (2).



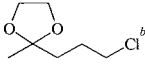
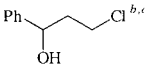
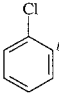
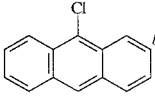
In a typical experiment (non Barbier-type) the organic halide in THF was slowly added over 20 min to a THF slurry of the polymer or metal oxide supported lithium naphthalenide at  $-78^\circ\text{C}$ . This resulted in the dissipation of the red colour of the supported lithium naphthalenide and the formation of an orange solution. After stirring for a further 1–3 h the mixture was filtered to give the arene free organoalkali species. In a typical Barbier-type experiment a mixture of the organic halide and source of electrophile in THF was slowly added over 45 min to a THF slurry of the polymer or metal oxide supported lithium naphthalenide at  $-30^\circ\text{C}$  or  $0^\circ\text{C}$ . The resulting pale yellow mixture was stirred for 15 min, filtered, hydrolysed, then extracted into  $\text{Et}_2\text{O}$ . Distillation afforded the corresponding quenched complex, free of arene or other by-products. In all cases, target concentrations of the resulting lithium reagent were close to 0.1 M.

Examples of lithium reagents prepared using polymers **6,6'** and a comparison with the use of lithium arene catalysed reactions are presented in Table 1. The yield of derived lithium reagents are high and comparable to those obtained in Refs. [7–18]. Each of the organic halides studied were quenched with chlorotrimethylsilane, and the resulting product characterised by  $^1\text{H}$  NMR and HPLC/MS.

The chlorinated dioxolane, **20**, was lithiated by the reaction with **6** in THF at  $-78^\circ\text{C}$ . Subsequent quenching with chlorotrimethylsilane afforded the corresponding silylated complex in high yield. The lithium reagent of the chlorohydrin, **21**, was obtained in high yield after **21** was pretreated with  $\text{LiBu}^n$  in THF at  $-10^\circ\text{C}$  to lithiate the alcohol residue, then treated with **6** at  $-78^\circ\text{C}$ . Quenching with chlorotrimethylsilane gave the bis-silylated complex in high yield. Alternatively, the chlorohydrin **21** can be di-lithiated directly using excess **6**. In this case the yield of the derived bis-silylated complex is reduced to 60%. For complexes **20** and **21**, an increase in reaction temperature resulted in decreased yields. This is presumably due to partial or total decomposition of the intermediates via proton abstraction from the solvent. However, when the reactions were carried out under Barbier-type conditions, slightly higher temperatures could be used with minimal effect on yields, viz. 92% for **20**,  $-78^\circ\text{C}$ , cf. 83%,  $-60^\circ\text{C}$ .

The lithium reagents of the arylchlorides, chlorobenzene **22** and 9-chloroanthracene **23** were obtained in

Table 1  
Comparison of the yield of lithium reagent using polymer supported lithium naphthalenide **6,6'**, with the use of lithium arene complexes (generated catalytically)

Organic Halide / Nitrile / Phosphate	% Yield of Lithium Reagent				literature
	<b>6</b>	<b>6'</b>	<b>28<sup>a</sup></b>		
	<b>20</b>	90	85	85	90 <sup>e,f</sup>
	<b>21</b>	80	75	85	89 <sup>e</sup>
	<b>22</b>	> 95	> 95	> 95	98 <sup>g</sup>
	<b>23</b>	> 95	> 95	> 95	> 95 <sup>h</sup>
MeCN <sup>d</sup>	<b>24</b>	50	50	55	39 <sup>i</sup>
PhCN <sup>d</sup>	<b>25</b>	75	70	70	63 <sup>i</sup>
(EtO) <sub>3</sub> PO <sup>d</sup>	<b>26</b>	85	80	85	90 <sup>j</sup>
(PhO) <sub>3</sub> PO <sup>d</sup>	<b>27</b>	95	90	90	87 <sup>j</sup>

<sup>a</sup> Reaction with lithium powder with 5% 1-(benzyltrimethylsilyl)naphthalene **28**.

<sup>b</sup> Reaction at  $-78^\circ\text{C}$ .

<sup>c</sup> Treated with  $\text{LiBu}^n$  (1.1 molar ratio,  $-10^\circ\text{C}$ ) prior to reaction with the lithium polymer.

<sup>d</sup> Reaction at  $-30^\circ\text{C}$ , Barbier-type reaction, isolated yield of distilled quenched product.

<sup>e</sup> Ref. [7,8].

<sup>f</sup> Ref. [9].

<sup>g</sup> Ref. [10].

<sup>h</sup> Reaction with lithium powder with 5% naphthalene (not from literature).

<sup>i</sup> Ref. [14].

<sup>j</sup> Ref. [13].

excellent yields, and quenching with chlorotrimethylsilane gave pure silylated derivatives. Changes in temperature had only slight effect on the yield of quenched products, viz. 62% for **23**,  $-40^\circ\text{C}$  cf. > 95%,  $-78^\circ\text{C}$ . For temperatures greater than  $-40^\circ\text{C}$  significant decreases in the yield were observed. Under Barbier-type conditions reaction temperatures of up to  $-25^\circ\text{C}$  for **23** still gave moderate yields, 58%.

The reaction of the nitriles **24**, **25** with **6** in THF at  $-30^\circ\text{C}$  in the presence of chlorotrimethylsilane, gave after hydrolysis tetramethylsilane and phenyltrimethylsilane respectively, in moderate yields. Reducing the

reaction temperature did not improve yields. Increasing the reaction temperatures on the other hand (to 0°C) reduced the yields slightly (by ca. 2–5%). The lower yield for **24** may be due to the high volatility of the quenched complex. In the work by Guijarro and Yus [14], lower yields of the target compound were attributed to the formation of by-products arising from preformed RLi deprotonating the unreacted nitrile. For example, the reaction of acetonitrile with benzaldehyde gave PhCH(OH)CH<sub>2</sub>CN. Other by-products were also isolated in these reactions including pinacol-type products [14]. Only the target complex and excess starting materials (< 5%) were isolated in the reactions in the present study (HPLC/MS).

Reaction of the trialkyl- **26** and triaryl- **27** phosphates with **6** in THF at –30°C in the presence of chlorotrimethylsilane, after hydrolysis led to the formation of ethyltrimethylsilane and phenyltrimethylsilane respectively in high yields. These products are being isolated upon distillation from reaction solvents. In these reactions, only one of the alkyl or phenyl groups of the starting phosphate is converted to the lithium reagent. The yields represent isolated yields after flash chromatography based on starting material. Changes in the reaction temperature such as an increase to 0°C, or decrease to –78°C, did not change the yield of product significantly. However, a decrease in the reaction temperature required an increase in reaction time, e.g. **26** reaction time at –78°C 3.5 h (80%), –30°C 2.5 h (85%), 0°C 1 h (75%).

Metal oxide supported lithium naphthalenides were also studied for their ability to form lithium reagents, Table 2. ‘Endcapping’ using chlorotrimethylsilane is inadequate whereas ‘endcapping’ using alane, as the trimethylamine adduct, H<sub>3</sub>Al · NMe<sub>3</sub>, gave a supported lithium complex effective in generating lithium reagents. The alane is more effective in removing residual hydroxyl groups and water, thus, giving the complexes more stability towards decomposition and loss of lithium (i.e., lithium reacts with the silica only to form the radical species and not with residual silanols or embed-

Table 2

Yield of lithium reagent derived from the reaction of metal oxide supported lithium naphthalene complexes, and recycled complexes

Metal oxide supported lithium naphthalenide	% Yield of lithium reagent <sup>a</sup>	
	Cycle 1	Cycle 2
<b>8</b>	80–85	78–83
<b>8'</b>	84–88	79–84
<b>9</b>	80–85	79–81
<b>9'</b>	82–85	79–83
<b>16</b>	50–56	40–44
<b>16'</b>	53–56	45–50
<b>17</b>	50–54	38–42
<b>17'</b>	51–58	40–49

<sup>a</sup>Range over three separate runs.

Table 3

Yield of sodium reagent derived from the reaction of polymer and metal oxide supported sodium naphthalene complexes and recycled complexes

Supported sodium naphthalenide	% Yield of sodium reagent <sup>a</sup>	
	Cycle 1	Cycle 2
<b>7</b>	85–95	75–80
<b>7'</b>	80–85	60–70
<b>12</b>	62–71	56–69
<b>12'</b>	63–71	60–67
<b>18</b>	37–50	22–35
<b>18'</b>	43–51	27–35
<b>19</b>	33–47	24–36
<b>19'</b>	37–49	30–39

<sup>a</sup>Range over three separate runs.

ded water). The lithium aminonaphthalenide complexes gave lower yields of the lithium reagents. The alumina and titania supported complexes in general gave lower yields of the organolithium reagents.

#### 2.4. Preparation of sodium reagents

The sodium supports were tested for their ability to form natriobenzene, Table 3. The polymer supported sodium naphthalenide is more effective than the corresponding metal oxide complexes. Reactions of the sodium polymer supports were carried out using the same procedure as described for the lithium analogues whereby a solution of the halide was added to a slurry of the support in THF at the –78°C. Addition of the halide resulted in the dissipation of the red colour of the supported complex and the formation of an orange solution of the sodium reagent which could be separated from the spent polymer by filtration.

The sodium supported complexes tend to be less stable than the corresponding lithium complexes, and not surprising they often decomposed during the addition of the reactant, resulting in reduced yields, or no sodium reagent formation. Similarly, the generated sodium reagent often decomposed prior to the reaction with the source of electrophile. It was therefore more successful to conduct these reactions under Barbier-type conditions which resulted in yields only slightly lower than those obtained from the lithium reagent. Decomposition of the reaction products most likely arises from proton abstraction from the solvent increasing with increasing temperature.

#### 2.5. Recycling of polymers and metal oxides

The spent polymers **3,3'** were tested for recycling potential. After quenching the polymers with chlorobenzene, the resulting lithium complex was filtered from the spent polymer. The polymer was then collected and washed with THF and loaded with lithium biphenylide

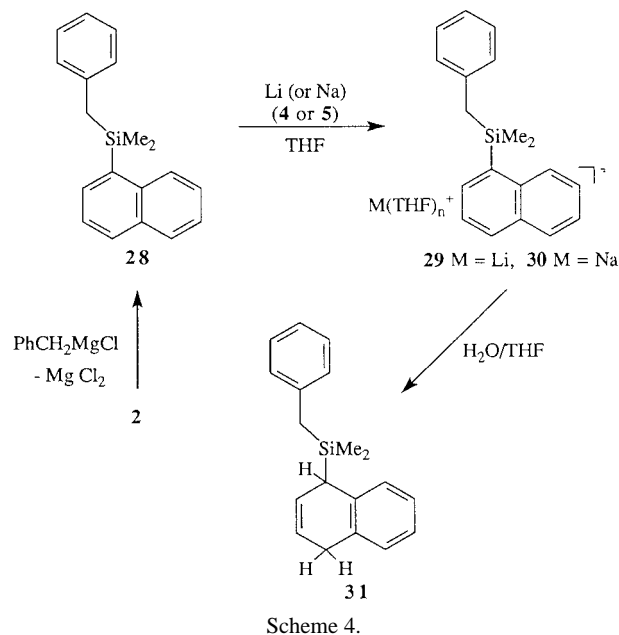
as before, yielding a deep red polymer, which was treated with chlorobenzene and the procedure repeated, Table 4. Overall, the uptake of **4** and the yield of lithium reagent obtained only differed slightly over successive cycles. The inability of the recovered polymers to consume the same amount of **4** as polymers in earlier cycles is due to 'poisoning' of the active sites within the polymer matrix through the formation of dihydroanthracene moieties. This could arise from proton abstraction by the radical anion centres from the solvent during washings to remove **4** (see below).

The spent metal oxide supports were tested for recycling ability, Tables 2 and 3. After quenching the polymers or metal oxide supported lithium or sodium naphthalenides with chlorobenzene, solutions of the resulting sodium complex were filtered from the macromolecule. The spent macromolecules were then reloaded with lithium or sodium, treated with chlorobenzene and the procedure repeated. Clearly metal oxide 'encapped' with alane is the preferred material for recycling purposes.

## 2.6. Model compounds

In an attempt to model the reaction of the functionalised polymers **3,3'** and **4,4'**, 1-(benzyl dimethylsilyl) naphthalene **28** was prepared by treating benzyl magnesium chloride with **2** in Et<sub>2</sub>O. Reaction of **28** with lithium or sodium metal yielded a deep green paramagnetic solution of Li{1-(benzyl dimethylsilyl)naphthalene}(THF)<sub>n</sub> **29**, (*g*<sub>av</sub> = 2.0028) and Na{1-(benzyl dimethylsilyl)naphthalene}(THF)<sub>n</sub> **30**, (*g*<sub>av</sub> = 2.0028), respectively, Scheme 4. Complexes **29** and **30** were also prepared by the reaction of **28** with THF solutions of **4** and **5** respectively. The reaction of **29** or **30** with chlorobenzene or 9-chloroanthracene both yielded the corresponding lithium or sodium complexes.

Treatment of the lithium or sodium naphthalenide complexes **29** or **30** with a solution of water in THF, Scheme 4, resulted in the formation of a dihydronaph-



thalene complex **31** which has been characterised by FTIR, HPLC/MS, and <sup>1</sup>H, <sup>13</sup>C, <sup>29</sup>Si NMR. This reaction models that of the polymer supported complexes, whereby treatment of the polymers **6,6'**, **7,7'** with water in THF results in the formation of a new material assigned as the dihydronaphthalene polymer **32,32'**, Eq. (3). Formation of dihydronaphthalene species is commonplace when alkali naphthalenides are treated with water or alcohols, or by proton abstraction from the reaction solvent [25]. Substituted (mono- or bis-) dihydronaphthalene complexes can also be formed upon reaction with alkyl halides [25].

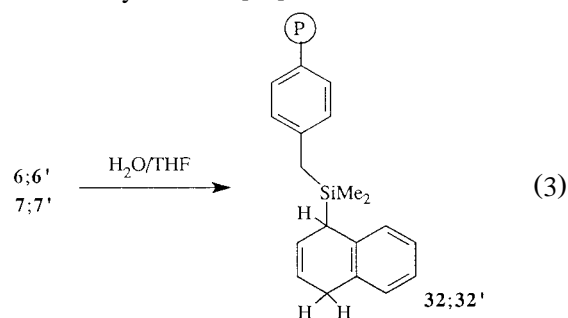


Table 4

Uptake of lithium biphenylide, **4**, by naphthalene functionalised polymers **3,3'** and yield of the lithium reagent from the subsequent reaction with chlorobenzene in THF at ca. -78°C, entry 1, and recycling of the recovered polymers, entry 2, and then repeating this process and recycling the recovered polymer, entry 3, etc.

Cycle	Addition of <b>4</b> (% theoretical)		% Lithium reagent formation <sup>a</sup>	
	<b>3</b>	<b>3'</b>	<b>3</b>	<b>3'</b>
1	110 <sup>b</sup>	110 <sup>b</sup>	93–97	93–95
2	100	95	91–95	89–95
3	100	95	89–94	87–93
4	95	90	88–92	87–92

<sup>a</sup> Range over three separate runs.

<sup>b</sup> > 100% added as a result of some hydrolysis.

## 2.7. Characterisation

All supported complexes were analysed using CP MAS NMR (<sup>13</sup>C and <sup>29</sup>Si), XPS, ESR and FTIR. NMR The <sup>29</sup>Si CP MAS NMR spectra of the naphthalene functionalised polymers **5** and the recycled material from the lithiation reaction are shown in Fig. 1. The spectra of **5** exhibits a single resonance at δ -3.9 ppm; a second resonance at δ +4.9 ppm is subsequently

observed on recycling which can be compared to the spectrum of **32**. The compound derived from the product of **6** and water and has a resonance at  $\delta +5.0$  ppm and a lower intensity resonance at  $\delta -3.9$  ppm, Fig. 1. The former is attributed to the silicon of the dihydronaphthalene, while the latter is attributed to unreacted starting material. Thus, for the recycled polymer the latter is indicative of the formation of dihydronaphthalene moieties. Similarly, for the higher loading polymer **5'** a single resonance is observed at  $\delta -3.5$  ppm, and a second resonance at  $\delta +4.7$  ppm in the spectra of the recycled material.  $^{29}\text{Si}$  CP MAS of **32'** shows two resonances, a dominant one at  $\delta +4.7$  ppm corresponding to the dihydronaphthalene polymer and a lower intensity resonance at  $\delta -3.4$  ppm corresponding to **5'**. The analogous spectra for recycled and water quenched polymers from the sodium complexes **7,7'** are the same as the lithium polymers, with differences in chemical shift of  $\leq 0.1$  ppm.

$^{29}\text{Si}$  CP MAS NMR has been used to identify the average structure of the surfaces by studying the shifts of the various substituents on surfaces [26–29]. Successive step in the preparation of metal oxide silylnaphthalene complexes, the reaction products were characterised by  $^{13}\text{C}$  and  $^{29}\text{Si}$  CP MAS NMR spectroscopy. Successive reactions are characterised by new resonances in both the  $^{13}\text{C}$  and  $^{29}\text{Si}$  CP MAS spectra as expected by the attached functional groups.

Chloropropyl functionalised silica has three distinct  $^{13}\text{C}$  NMR resonances at  $\delta 10.0$ ,  $26.5$ , and  $46.0$  ppm

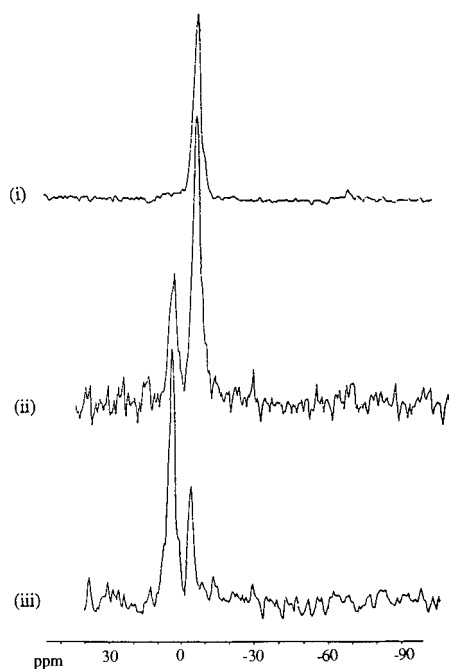


Fig. 1.  $^{29}\text{Si}$  CP MAS NMR spectra of (i) naphthalene functionalised polymer **3**, (ii) polymer **3** after being recycled two times, (iii) dihydronaphthalene polymer **32**.

corresponding to the methylene carbon centres [29,30]. A  $^{29}\text{Si}$  NMR resonance at  $\delta -45$  to  $-70$  ppm corresponds to the silicon bearing the propyl group. Subsequent trimethylsilyl 'endcapping' generates a new resonance at  $\delta 8.0$  ppm, as well as a new resonance in the  $^{13}\text{C}$  NMR spectrum at  $\delta -0.1$  ppm [24]. Functionalisation with silylnaphthalene generates a broad aromatic resonance at  $\delta 127.9$  ppm with reduction in the resonance at  $\delta 46.0$  ppm (residual unreacted  $\text{ClCH}_2$ -groups), Fig. 2. A large resonance at  $\delta 17.3$  ppm is assigned to the carbons attached to the silicon functionality,  $-\text{CH}_2\text{SiMe}_3$ . Similarly, a new small resonance in the  $^{29}\text{Si}$  NMR spectrum at  $\delta 10$  ppm is due to this silicon functionality. This resonance is not always seen, the intensity depending on a variety of factors including loading level, NMR collection time and signal to noise ratio.

Similar results were obtained for the corresponding alumina and titania silylnaphthalene supports. Resonances assigned to the functionalities on the support in the  $^{13}\text{C}$  CP MAS NMR for the alumina and titania complexes did not shift significantly compared to the silica derivatives. For many of the complexes, however, the signal corresponding to the trimethylsilyl 'endcapping' was either very small, or could not be detected. Similarly, the resonances assigned to the aromatic carbons of the naphthalene functionality were very weak for the titania complexes. Shifts corresponding to the functionality in the  $^{29}\text{Si}$  CP MAS NMR for the alumina and titania complexes did not shift significantly compared to the silica derivatives.

Aminonaphthalene silica has four different carbons corresponding to the silylating agent [31], which were easily identified in the  $^{13}\text{C}$  NMR spectrum at  $\delta 10.3$ ,  $20.7$ ,  $34.3$ ,  $52.6$  ppm, with a broad resonance at  $\delta 130.9$  representing the aromatic functionality.  $^{29}\text{Si}$  NMR resonances were at  $\delta -50$  to  $-75$  ppm. A separate  $^{13}\text{C}$  NMR resonance for the methylene group attached to naphthalene was not evident, and most likely coincides with the N-Me resonance at  $\delta 34.3$  ppm. Subsequent trimethylsilyl 'endcapping' generated new resonances at  $\delta 0.2$  ppm ( $^{13}\text{C}$  NMR) and  $\delta 10.2$  ppm ( $^{29}\text{Si}$  NMR). These signals are often very small or absent in the spectrum, especially for the alumina and titania complexes.

## 2.8. XPS

Selective information could be obtained from the data, including elemental percentages, chemical binding onto the metal oxide and mode of adsorption of alane and gallane species. More detailed analysis of peak shape and atomic concentration ratios led to information about the position and number of different types of atoms within the molecule. The binding energies of

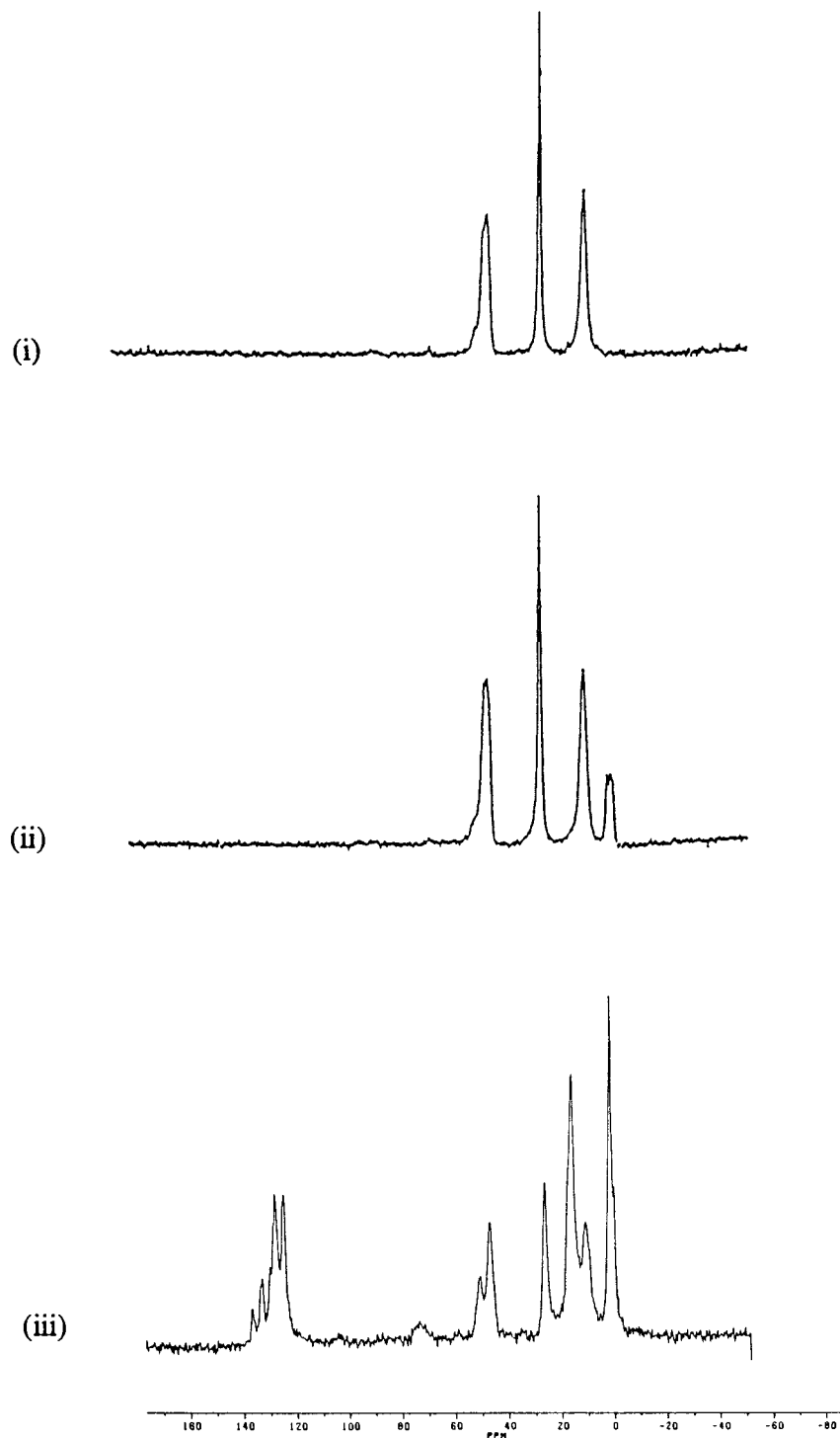


Fig. 2.  $^{13}\text{C}$  CP MAS NMR spectra of (i) chloropropyl silica, (ii) trimethylsilyl 'endcapped' chloropropyl silica, (iii) trimethylsilyl 'endcapped' silylnaphthalene silica.

each of the elements change only slightly irrespective of the synthetic step applied to the metal oxides. Similar results have been obtained by other groups [32–36].

Elemental analyses were calculated using experimentally determined sensitivity factors [37]. In all cases the elemental analyses were normalised to 100%. The trends

in the ratios of elemental atomic concentrations is in the expected range and is in agreement with the desired change in functionalisation at each step in the synthetic pathways described. Fig. 3 shows the principal photoelectron peaks (C 1s, O 2p, Si 1s, Cl 2p, Al 2p and N 1s) for trimethylsilyl and trimethylamine alane 'en-



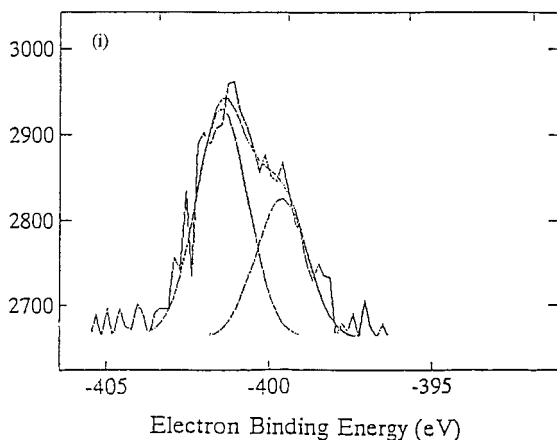


Fig. 3. Curve-fitted N 1s photoelectron peak for trimethylsilyl and alane 'endcapped' chloropropyl silica.

dcapped' chloropropyl silica. The O 1s and Si 2p photoelectron peaks are symmetric and occur at  $E_B = 533.0$  and  $103.8$  eV, respectively and are characteristic of  $\text{SiO}_2$ . The Al 2p photoelectron peak is broad and symmetric and occurs at  $E_B = 75.7$  eV, and is consistent with  $\text{Al}^{\text{III}}$  or Al–O species [32,33]. The C 1s and N 1s show multi species character. Multiple species are expected from the carbon, as it is made up of the propyl carbons, trimethylamine carbons and adventitious carbon on the silica surface. Curve fitting of the N 1s peak indicated that at least two different nitrogen species are present on the surface, at  $E_B = 399.2$  and  $401.5$  eV, Fig. 4.

Surface adsorption characteristics of  $\text{H}_3\text{Al} \cdot \text{NMe}_3$  on a  $\text{SiO}_2$  substrate have been investigated using X-ray photoelectron spectroscopy (XPS) and static secondary

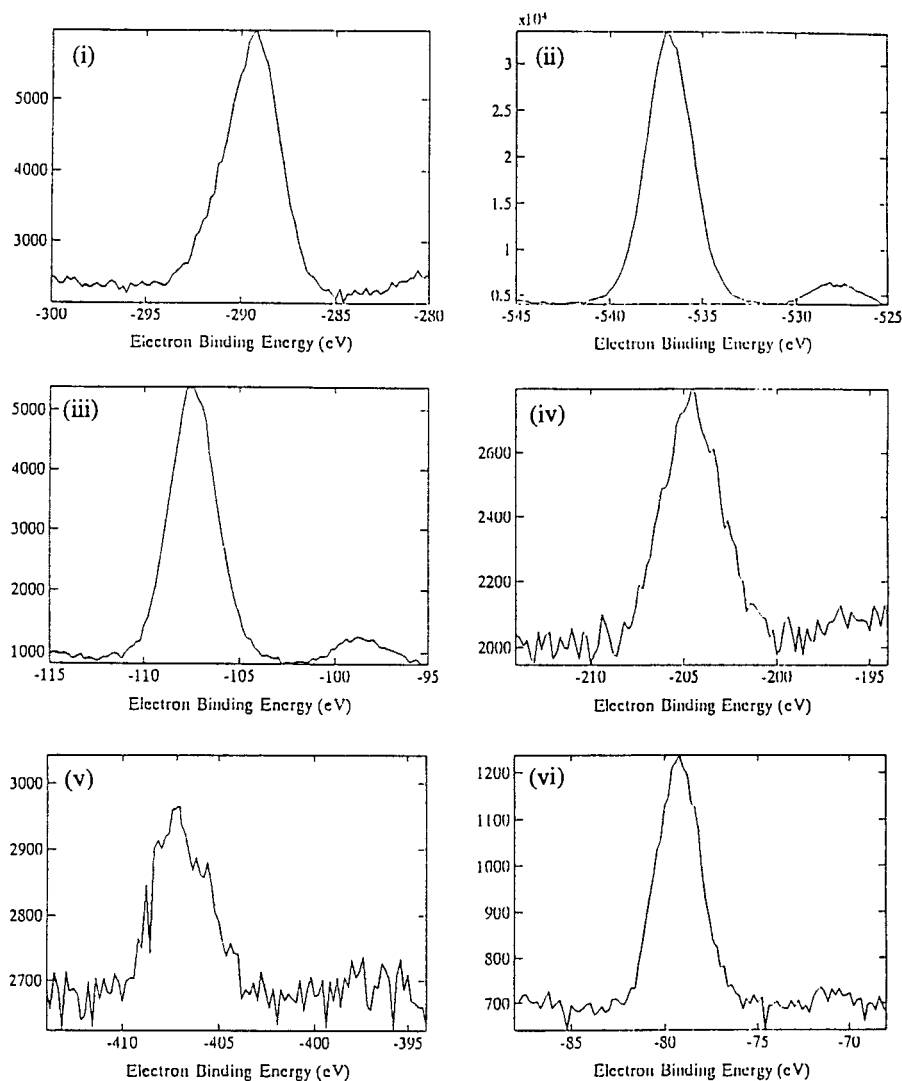


Fig. 4. X-ray Photoelectron spectra of trimethylsilyl and alane 'endcapped' chloropropyl silica powder (i) C 1s, (ii) O 1s, (iii) Si 2p, (iv) Cl 2p, (v) N 1s, (vi) Al 2p.

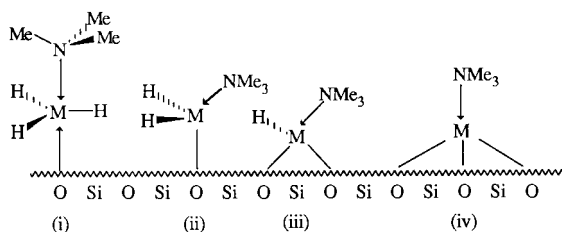


Fig. 5. (i) Molecularly adsorbed trimethylamine alane (gallane),  $\text{Si}_2\text{OMH}_3\text{NMe}_3$  (5-coordinate). (ii) Chemisorbed trimethylamine alane (gallane),  $-\text{OMH}_2\text{NMe}_3$  (4-coordinate). (iii) Chemisorbed trimethylamine alane (gallane),  $-\text{O}_2\text{MHNMe}_3$  (4-coordinate). (iv) Chemisorbed trimethylamine alane (gallane),  $-\text{O}_3\text{MNMe}_3$  (4-coordinate).

ion mass spectrometry (SSIMS) [38,39]. In this study, the N 1s peak was deconvoluted into two component peaks ( $E_B = 399.2$  and  $402$  eV) [38,39]. The higher binding energy component was attributed to nitrogen from molecularly adsorbed trimethylamine alane (forming a 5-coordinate aluminium centre (i)), and the lower binding energy to the adsorption of free trimethylamine [38,39]. These assignments were confirmed by analysis of SSIMS data, and by the dosing of aluminium and oxidised silicon substrates with trimethylamine [38,39]. Fig. 5 represents the possible bonding modes of trimethylamine alane ( $\text{M}=\text{Al}$ ) or gallane ( $\text{M}=\text{Ga}$ ).

In the present study, the lower binding energy at  $399$  eV can be attributed to molecularly bound trimethylamine. The second component at  $401.5$  eV can be attributed to the nitrogen from chemically bound trimethylamine alane in the form of partially oxidised aluminium hydrides (ii) {(iii) or (iv)},  $-\text{OAlH}_2\text{NMe}_3$ . In this case, the aluminium is now in a 4-coordinate environment, and a slight shift in the binding energy would be expected. Preliminary investigations into the analysis of the surface species by secondary ion mass spectrometry showed that a large population of  $\text{AlH}_2^+$  species existed, as indicated by a large peak at  $29$  amu. Further evidence for the existence of this 4-coordinate species is achieved by the analysis of the FTIR spectra.

In an attempt to further identify  $-\text{OAlH}_2\text{NMe}_3$  and  $=\text{OAlH}_3\text{NMe}_3$  species on the silica surface, trimethylamine alane was physisorbed on silica. Silica powder and trimethylamine alane were stirred together for 3 h under vacuum, in an attempt to mimic dosing experiments of Elms et al. [38,39] and Simmonds et al. [40]. The surface adsorption characteristics of the resultant substrate were investigated using XPS and SSIMS. As expected, similar results to these earlier studies were obtained, such that molecularly adsorbed trimethylamine and trimethylamine alane were present as surface species [38–40].

Analysis of the N 1s photoelectron peak of trimethylamine alane ‘endcapped’ alumina were inconclusive as

to the type and number of nitrogen species present; a broad peak ranging from  $E_B = 399.5$  to  $404$  eV was obtained. This is possibly made up of two peaks at  $E_B = 401$  and  $402$  eV. Only slight changes in the binding energies of the surface species was expected, making interpretation difficult. The peaks could possibly be attributed to the nitrogens of  $-\text{OAlH}_2\text{NMe}_3$  and  $-\text{O}_3\text{AlNMe}_3$  respectively. The N 1s photoelectron peak of aluminium foil dosed with trimethylamine occurs at  $E_B = 402$  eV, and is assigned to trimethylamine molecularly adsorbed [41]. Similarly, the peak at  $402$  eV for the alumina complex can be assigned to the nitrogen of molecularly adsorbed trimethylamine. As only weak signals were obtained for the N 1s photoelectron peak analysis of trimethylamine alane ‘endcapped’ titania species is inconclusive to the type and number of nitrogen species present.

Similar analysis of the principal photoelectron peaks (C 1s, O 2p, Si 1s, Cl 2p, Ga  $2p_{3/2}$  and N 1s) for trimethylsilyl and trimethylamine gallane ‘endcapped’ chloropropyl silica were investigated. The O 1s and Si 2p photoelectron peaks are symmetric and occur at  $E_B = 533.0$  and  $103.8$  eV, respectively and are characteristic of  $\text{SiO}_2$ . The Ga  $2p_{3/2}$  photoelectron peak is broad and symmetric and occurs at  $E_B = 1119.8$  eV, and is consistent with  $\text{Ga}^{\text{III}}$  or  $\text{Ga}-\text{O}$  species [32]. The C 1s and N 1s show multi species character. Analysis of the N 1s peak for trimethylamine gallane ‘endcapped’ species suggested that the trimethylamine is molecularly adsorbed onto the metal oxide surface and is also molecularly bound to the gallium metal centres. The N 1s peak is broad and centred around  $E_B = 401.7$  eV. Peak shape analysis reveals two possible component peaks at approximately  $E_B = 395.5$  and  $402.3$  eV, which can be assigned to the nitrogens of molecularly adsorbed trimethylamine, and chemically adsorbed trimethylamine gallane. Alumina and titania N 1s photoelectron peaks were too small and noisy to be deconvoluted in the similar manner.

The surface adsorption characteristics of  $\text{H}_3\text{Ga} \cdot \text{NMe}_3$  on an  $\text{SiO}_2$  substrate has been investigated using XPS and SSIMS by Butz et al. [42]. The N 1s peak is axially symmetric and low in intensity ( $E_B = 400$  eV) [42]. The intensity of the peak decreased with time in the vacuum chamber, indicating that the adsorbed nitrogen species readily desorbs from the surface. The peak was assigned to the nitrogen from the adsorption of trimethylamine onto the substrate surface. SSIMS data were also consistent with this assignment [42]. Molecular adsorption of trimethylamine gallane would require the formation of a 5-coordinate gallium species, which are highly unstable (see below), as gallium prefers to be in a 4-coordinate environment. Low temperature dosing ( $-190^\circ\text{C}$ ) of trimethylamine gallane onto a  $\text{SiO}_2$  wafer was also investigated [42]. The N 1s peak in this case deconvoluted into two component peaks at  $E_B = 402.4$

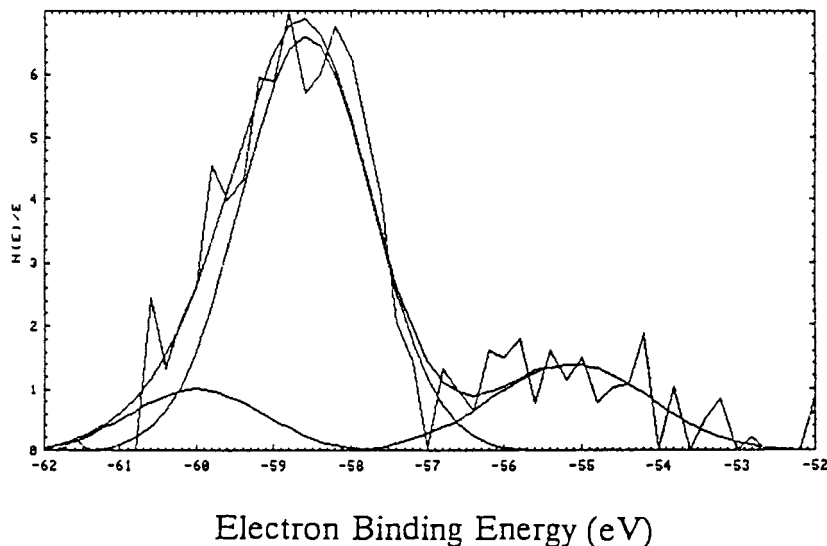


Fig. 6. Curved fitted X-ray Photoelectron spectrum of Li 1s of trimethylsilyl 'endcapped' lithiopropyl silica.

and 400 eV, attributed to molecularly adsorbed  $\text{H}_3\text{Ga} \cdot \text{NMe}_3$  and  $\text{NMe}_3$ , respectively.

In the present study the N 1s peak was deconvoluted into two component peaks  $E_B = 402.3$  and  $395.5$  eV, assigned to the nitrogens of chemisorbed  $\text{H}_3\text{Ga} \cdot \text{NMe}_3$  and molecularly adsorbed  $\text{NMe}_3$ . The gallium species is expected to be 4-coordinate. Five-coordinate gallium species are in general unstable, for example  $\text{H}_3\text{Ga} \cdot (\text{NMe}_3)_2$  decomposes  $< -26^\circ\text{C}$  to  $\text{H}_3\text{Ga} \cdot \text{NMe}_3$  [43]. FTIR is in agreement with these findings (see below).

Analysis of the Li 1s photoelectron peak of trimethylsilyl lithiopropyl silica shows multi species character, Fig. 6. Asymmetry of the Li 1s peak arising a high binding energy tail is due to the presence of Li–C species. The low binding energy component is not a Li 1s species, but a C 1s ghost peak from stray Al– $\text{K}_\alpha$  radiation (233 eV lower than C 1s) from the X-ray source, Fig. 6ii. This is therefore in agreement with the suggested formation of 'OLi' species on the surface of the silica, during the reaction of lithium biphenylide with the chloropropyl supported complexes.

## 2.9. FTIR

At each successive step in the preparation of the metal oxide complexes, the reaction products and starting materials were characterised by FTIR as a method of determining if residual hydroxyl groups were present. For alane and gallane 'endcapped' complexes, absorbances attributable to residual Al–H and Ga–H groups were present at  $1870$  and  $1970$   $\text{cm}^{-1}$  respectively. As expected the values of these complexes are at a higher wavelength than the corresponding free metal trihydride. A comparison of free metal hydride physisorbed and chemisorbed metal hydride is given in Table 5, and there is a change in the environment of the

metal hydride, suggesting the formation of mono- and di-hydridometal species.

Simmonds et al. [40] have studied the absorption of dimethylethylamine alane onto an oxidised silicon surface, and characterised the surface species by FTIR spectroscopy. In their study, a change in the IR absorption band for Al–H was observed from  $1780$  to  $1850$   $\text{cm}^{-1}$  upon adsorption. The peak at  $1780$   $\text{cm}^{-1}$  is attributed to the hydrides of physisorbed (molecularly bound) dimethylethylamine alane. Partially oxidised aluminium hydrides, formed from the chemisorption of dimethylethylamine alane on the silica surface generates a new peak at  $1850$   $\text{cm}^{-1}$ . Heating to  $145^\circ\text{C}$  during dosing on the surface resulted in even higher values of the hydride shift. This is expected to be due to the decomposition of dihydrido species and the subsequent formation of mono-hydride species of aluminium oxide. The higher value of the Al–H absorbances is consistent with the formation of a 4-coordinate aluminium oxide species, e.g.,  $\text{H}_2\text{Al}(\text{NMe}_3)\text{OSiO}_3$  and  $\text{HAl}(\text{NMe}_3)(\text{OSiO}_3)_2$  type species.

In the present study, physisorbed  $\text{H}_3\text{Al} \cdot \text{NMe}_3$  has

Table 5  
M–H stretching frequencies

Compound/material	$\nu(\text{M–H})$ ( $\text{cm}^{-1}$ )
$\text{H}_3\text{AlNMe}_3$	1760
physisorbed alane on silica	1790
chemisorbed alane on silica	1890
chemisorbed alane on alumina	1890
chemisorbed alane on titania	1875
$\text{H}_3\text{GaNMe}_3$	1855
physisorbed gallane on silica	1860
chemisorbed gallane on silica	1980
chemisorbed gallane on alumina	1985

an absorbance assigned to the Al–H frequency at  $1790\text{ cm}^{-1}$ , and the chemisorbed species at  $1870\text{ cm}^{-1}$ . The absorbance value of the chemisorbed species would suggest the formation of a dihydro–aluminium oxides surface species, when compared to values observed by Simmonds et al. [40]. Absorbances of aluminium hydride alkoxide species supports this theory [44–47]. A number of alkoxide aluminium hydrides have been prepared, each having slight different absorbances attributed to the Al–H of the complex. The complexes  $(i\text{-C}_4\text{H}_9\text{OAlH}_2)_2$ ,  $(t\text{-C}_4\text{H}_9\text{O})_2\text{AlH}$  and  $(t\text{-C}_4\text{H}_9\text{O})\text{AlH}_2$  have hydride absorbances at 1842, 1859 and  $1842\text{ cm}^{-1}$ , respectively. Similarly, a variety of amine alkoxide aluminium hydrides also have different absorbances attributed to the Al–H, including  $\text{AlH}_2(\text{OR})(\text{NMe}_3)$   $1800\text{--}1900\text{ cm}^{-1}$ ,  $[\text{AlH}_2(\text{OR})(\text{NMe}_3)]_2$ ,  $\text{AlH}_2(\text{OR})_2(\text{NH}_2\text{Bu}^t)$   $1867\text{ cm}^{-1}$ ,  $\text{AlH}_2(\text{OR})_2(\text{OEt}_2)$   $1896\text{ cm}^{-1}$ , for  $\text{R} = \text{C}_6\text{H}_2\text{Bu}^t\text{-2,6-Me-4}$  [46–48], and  $[\{\text{H}_2\text{Al}(\mu\text{-OC}(\text{H})\text{Bu}^t)_2\}_2\text{AlH}(\mu\text{-H})_2]$   $1868\text{ cm}^{-1}$  [49].

Similarly, higher shifts in the Ga–H species can also be attributed to the formation of partially oxidised species. In fact, as discussed in the XPS section the gallium is most likely in a 4-coordinate environment. Gallium hydride shifts for alkoxide complexes have higher values for the Ga–H stretch. For example  $[\text{H}_2\text{Ga}(\mu\text{-OC}(\text{H})\text{Bu}^t)_2]_2$   $1918\text{ cm}^{-1}$  [49].

Another important feature of the IR spectra of the metal oxides ‘endcapped’ with aluminium hydride is the formation of a new absorbance band at  $2000\text{ cm}^{-1}$  which can be attributed to Si–H, Fig. 7. The Si–H species is either formed from the decomposition of Al–H and the subsequent reaction with siloxanes generating a Si–H species, as suggested by Simmonds et al. [40], or the hydrides may be formed in situ with a dihydroaluminium oxide species. Similar species were not detected in the gallium ‘endcapped’ samples, Fig. 8. This is likely to be due to the high stability of the gallium surface species, and this is evident by its stability in air (see below).

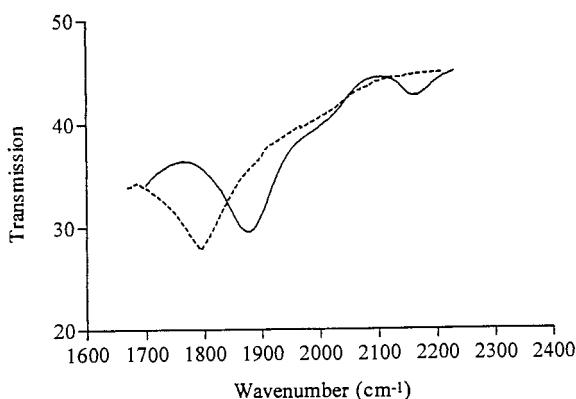


Fig. 7. FTIR spectra of the Al–H and Si–H stretching regions of (i) physisorbed alane (---), (ii) chemisorbed alane (—).

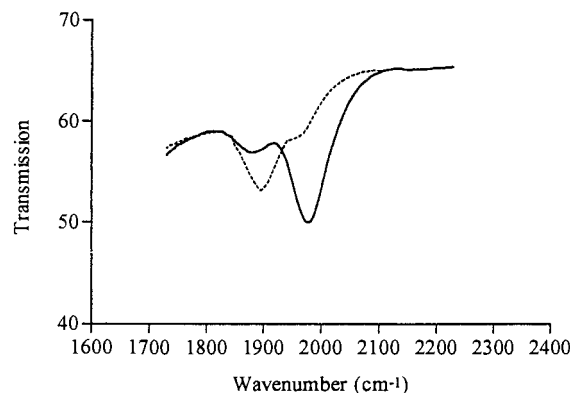


Fig. 8. FTIR spectra of the Ga–H and Si–H stretching regions of (i) physisorbed gallane (---), (ii) chemisorbed gallane (—).

Analysis of changes in the spectra of trimethylamine alane and gallane when exposed to air indicate the stability of the surface protecting groups. The gallane species proved to be more stable with respect to oxidation in air. Decomposition of the alane complexes results in the loss of a band attributable to the Al–H, and the formation of an absorbance attributable to a hydroxyl group. This process was complete within a 10 min air exposure, compared with a 40 min exposure for the gallane complex.

## 2.10. EPR

The EPR spectra of the polymer supported alkali naphthalenides **6** and **7** were obtained at room temperature in THF. The EPR spectrum of **6** and a simulated spectrum are given in the preliminary account of this work [1]. The spectrum appears as a multiplet ( $g_{av} = 2.00275$ ) with hyperfine coupling. Simulation using SOPHE [50] indicated the multiplet was generated from the coupling of two equivalent lithiums ( $A(^7\text{Li}) = 2.489 \pm 0.004\text{ G}$ ), four equivalent hydrogens ( $A(^1\text{H}) = 1.401 \pm 0.002\text{ G}$ ) and two other equivalent hydrogens

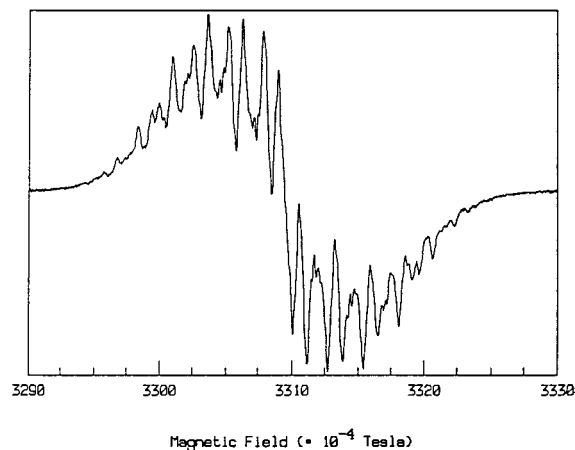


Fig. 9. EPR spectra of polymer supported sodium naphthalenide **7**.

(A ( $^1\text{H}$ ) =  $2.593 \pm 0.004$  G). Several simulation experiments were carried out for various couplings, including Li–Li, Li–H, of varying combinations of atoms, and numbers of equivalent atoms (for example  $6 \times \text{Li}$ ,  $4 \times \text{Li}$ , and  $4 \times \text{Li}$  with  $4 \times \text{H}$ ). The best fit was obtained for the system described above.

The EPR spectrum of polymer supported sodium naphthalenide also gave a multiplet with hyperfine coupling (Fig. 9). In this case there is a broadening of the signals making simulation difficult. The broadening may arise from dipole–dipole interaction of the sodium atoms which has been seen in sodium zeolite systems [51,52].

### 3. Experimental section

Silica gel, Keisegel 60, 230 mesh was purchased from Fluka. Alumina used was laboratory grade for column chromatography, activity grade 1, basic, and was obtained from Sigma (A-8878). Titania (GPR 30446) was obtained from BDH Chemicals. Chloromethylated polystyrene (1.20–1.34, and 4.11–4.15 mmol  $\text{g}^{-1}$  Cl) was purchased from BIO-RAD. LiBu<sup>n</sup> was obtained from Metallgesellschaft (Germany) as a hexane solution, typically 1.60 M, and was standardised before use. Benzonitrile, 1-bromo-naphthalene, 9-chloroanthracene, 1-chloromethylnaphthalene, 5-chloro-2-pentanone, 3-chloro-1-phenyl-1-propanol, 3-(chloropropyl)trimethoxysilane, triethylphosphate and triphenylphosphate were obtained from Aldrich. *N*-Methyl(3-aminopropyl)trimethoxysilane was purchased from Petrach chemicals. 1-(Chlorodimethylsilyl)naphthalene [22],  $\text{H}_3\text{Al} \cdot \text{NMe}_3$  [53],  $\text{H}_3\text{Ga} \cdot \text{NMe}_3$  [54],  $\text{Mg}(\text{anthracene})(\text{THF})_3$  [55], lithium and sodium biphenylide [56] were prepared following literature procedures. Lithium powder dispersed in paraffin, was washed in hexane and dried prior to use. 2-(3'-Chloropropyl)-2-methyl-1,3-dioxalane was prepared from 5-chloro-2-pentanone following standard literature procedures [57].

#### 3.1. Synthesis of 1-(chlorodimethylsilyl)naphthalene 2 [22]

A hexane solution of LiBu<sup>n</sup> (55 ml, 84 mmol) was added to an ice-cooled solution of 1-bromonaphthalene (16.5 g, 80 mmol) in  $\text{Et}_2\text{O}$  (100 ml) over 10 min. The resulting orange solution was stirred for 1 h at room temperature during which time an orange precipitate formed. The mixture was then added dropwise to a solution of dichlorodimethylsilane (15 ml, 123 mmol) in  $\text{Et}_2\text{O}$  (50 ml), over 15 min at  $-78^\circ\text{C}$ , and the reaction mixture stirred overnight, warming to room temperature. Volatiles were then removed in vacuo, the residue taken up in hexane (100 ml), and the solution filtered to remove lithium chloride. Volatiles were then removed

in vacuo and the resulting brown oil was distilled affording a colourless liquid of the title compound (11.5 g, 66%), b.p.  $120^\circ\text{C}$  (0.5 mmHg).  $^1\text{H}$  NMR: (250 MHz,  $\text{CDCl}_3$ ),  $\delta$  0.6 (s,  $\text{SiMe}_2$ ), 7.10–7.35 (3H, m,  $\text{H}_{3,6,7}$ ), 7.53–7.74 (3H, m,  $\text{H}_{4,5,8}$ ), 8.33 (1H, m,  $\text{H}_2$ );  $^{13}\text{C}$  NMR: (62.8 MHz,  $\text{CDCl}_3$ ),  $\delta$  3.5 ppm ( $\text{SiMe}_2$ ), 125.3 ( $\text{C}_6$ ), 126.1 ( $\text{C}_7$ ), 126.7 ( $\text{C}_3$ ), 128.1 ( $\text{C}_8$ ), 129.7 ( $\text{C}_5$ ), 131.8 ( $\text{C}_4$ ), 134.2 ( $\text{C}_2$ ), 134.3 ( $\text{C}_{4a}$ ), 136.5 ( $\text{C}_{1a}$ ), 139.1 ( $\text{C}_1$ );  $^{29}\text{Si}$  NMR (59.61 MHz),  $\delta$   $-26.3$  ppm (s,  $\text{SiMe}_2$ ). IR (thin film)  $\nu(\text{Si}-\text{C})$   $850\text{ cm}^{-1}$ .

#### 3.2. Synthesis of naphthalene functionalised polymers 3,3'

A solution of 1-(chlorodimethylsilyl)naphthalene, **2** [(a) 1.67 g, 7.57 mmol; (b) 3.5 g, 15.8 mmol] in THF (50 ml) was added to an ice-cold slurry of the Grignard reagent of chloromethylated polystyrene [(a) 7.0 g, 1.34 mmol  $\text{g}^{-1}$ , 7.57 mmol; (b) 6.52 g, 4.11 mmol  $\text{g}^{-1}$ , 15.8 mmol] in THF (100 ml). The reaction mixture was stirred for 12 h at room temperature. The modified polymer was filtered, washed with THF ( $3 \times 75$  ml) and dried in vacuo for 6 h at  $60^\circ\text{C}$  to afford compound **3,3'** as a white solid [(a). 6.8 g, 99%; (b). 6.2 g, 100% based on weight gain]. (Found for **3** C, 89.2; H, 8.4; Cl,  $<0.3\%$ , **3** requires C and H 96.87, Cl 0%). (Found for **3'** C, 88.1; H, 7.9; Cl 0.2%, **3'** requires C and H 92.86; Cl, 0%).  $^{29}\text{Si}$  NMR (79.45 MHz, CP MAS):  $\delta$   $-3.9$ ,  $-3.5$ . IR (nujol):  $\nu(\text{C}-\text{H})$  1251, 1253  $\text{cm}^{-1}$   $\nu(\text{Si}-\text{C})$  844, 839  $\text{cm}^{-1}$ .

#### 3.3. Synthesis of polymer supported lithium naphthalenide 6,6'

A slurry of silylnaphthalene polymer **3,3'** [(a) 2.8 g, 3.13 mmol; (b) 2.0 g, 5.09 mmol] in THF (50 ml) was stirred for 12 h at room temperature. A solution of lithium biphenylide **4** [1.5 M, (a) 2.2 ml, 3.3 mmol; (b) 3.6 ml, 5.4 mmol] in THF was added slowly to the swollen polymer affording a deep blue mixture. This was stirred for 12 h resulting in a reddish-brown solid. The filtrate was removed, the polymer was washed with THF ( $3 \times 50$  ml) and dried in vacuo for 6 h to afford compound **6,6'** as a red/brown solid [(a) 2.8 g; (b) 2.0 g]. EPR  $g_{\text{av}} = 2.0029, 2.0026$ .

#### 3.4. Synthesis of polymer supported sodium naphthalenide 7,7'

A slurry of silylnaphthalene polymer **3,3'** [(a) 3.7 g, 4.1 mmol; (b) 1.5 g, 3.8 mmol] in THF (50 ml) was stirred for 12 h at room temperature. A solution of sodium biphenylide **5** [1.5 M, (a) 2.9 ml, 4.4 mmol; (b) 3.5 ml, 4.7 mmol] in THF was added slowly to the swollen polymer affording a deep blue mixture. This was stirred for 12 h resulting in a reddish-brown solid.

The filtrate was removed and the polymer was washed with THF (3 × 50 ml) and dried in vacuo for 6 h to afford compound **7,7'** as a red/brown solid [(a) 3.6 g; (b) 1.5 g]. EPR  $g_{av} = 2.0033, 2.0100$ .

### 3.5. Synthesis of alane 'endcapped' silica supported silylnaphthalene **8**

To a suspension of lithiopropyl trimethylsilyl and alane 'endcapped' silica (derived from the reaction of lithium biphenylide with chloropropyl trimethylsilyl and alane 'endcapped' silica (1.2 g) was added 1-(chlorodimethylsilyl)naphthalene (0.5 g) and the pale yellow mixture stirred overnight. Powder **8** was filtered and washed with THF then dried in vacuo at 60°C for 6 h (1.2 g).  $^{29}\text{Si}$  NMR (79.45 MHz, CP MAS)  $\delta$  -100 to -120 (lattice silicon), -50 to -75 (OSiCH<sub>2</sub>), 10.5 (Si(CH<sub>3</sub>)<sub>3</sub>), 0.0 (Si(CH<sub>3</sub>)<sub>2</sub>);  $^{13}\text{C}$  NMR (100.56 MHz, CP MAS):  $\delta$  2.3 (Si(CH<sub>3</sub>)<sub>3</sub>), 11.8 (CH<sub>2</sub>Si), 17.2 (CH<sub>2</sub>SiCH<sub>3</sub>), 26.0 (CH<sub>2</sub>CH<sub>2</sub>CH<sub>2</sub>), 47.8 (small peak, CH<sub>2</sub>Cl), 127.2 (C<sub>arom</sub>). IR (nujol)  $\nu(\text{Al-H})$  1879 cm<sup>-1</sup>. [**8'**  $^{29}\text{Si}$  NMR (79.45 MHz, CP MAS)  $\delta$  -90 to -120 (lattice silicon), -40 to -65 (OSiCH<sub>2</sub>), 9.5 (Si(CH<sub>3</sub>)<sub>3</sub>), (Si(CH<sub>3</sub>)<sub>2</sub>) (not detected);  $^{13}\text{C}$  NMR (100.56 MHz CP MAS)  $\delta$  2.0 (Si(CH<sub>3</sub>)<sub>3</sub>), 11.3 (CH<sub>2</sub>Si), 17.1 (CH<sub>2</sub>SiCH<sub>3</sub>), 27.0 (CH<sub>2</sub>CH<sub>2</sub>CH<sub>2</sub>), 47.8 (small peak, CH<sub>2</sub>Cl), 128.0 (C<sub>arom</sub>). IR (nujol):  $\nu(\text{Ga-H})$  1980 cm<sup>-1</sup>.

### 3.6. Synthesis of alane 'endcapped' silica supported silylnaphthalene **9**

To a suspension of lithiopropyl alane 'endcapped' silica (derived from the reaction of lithium biphenylide with chloropropyl alane 'endcapped' silica (0.5 g)) was added 1-(chlorodimethyl)silylnaphthalene (0.2 g) and the pale yellow mixture stirred overnight. Powder **9** was filtered and washed with THF then dried in vacuo at 60°C for 6 h (0.5 g).  $^{29}\text{Si}$  NMR (79.45 MHz, CP MAS)  $\delta$  -100 to -125 (lattice silicon), -50 to -80 (OSiCH<sub>2</sub>), 1.0 (Si(CH<sub>3</sub>)<sub>2</sub>);  $^{13}\text{C}$  NMR (100.56 MHz, CP MAS)  $\delta$  11.5 (CH<sub>2</sub>Si), 18.0 (CH<sub>2</sub>SiCH<sub>3</sub>), 28.0 (CH<sub>2</sub>CH<sub>2</sub>CH<sub>2</sub>), 48.0 (small peak, CH<sub>2</sub>Cl), 128.8 (C<sub>arom</sub>). IR (nujol):  $\nu(\text{Al-H})$  1876 cm<sup>-1</sup>. [**9'**  $^{29}\text{Si}$  NMR (79.45 MHz, CP MAS)  $\delta$  -90 to -125 (lattice silicon), -40 to -80 (OSiCH<sub>2</sub>), 0.7 (Si(CH<sub>3</sub>)<sub>2</sub>);  $^{13}\text{C}$  NMR (100.56 MHz, CP MAS)  $\delta$  11.5 (CH<sub>2</sub>Si), 17.8 (CH<sub>2</sub>SiCH<sub>3</sub>), 26.9 (CH<sub>2</sub>CH<sub>2</sub>CH<sub>2</sub>), 47.9 (small peak, CH<sub>2</sub>Cl), 128.2 (C<sub>arom</sub>). IR (nujol)  $\nu(\text{Ga-H})$  1979 cm<sup>-1</sup>.

### 3.7. Synthesis of alane and trimethylsilyl 'endcapped' silica supported lithium naphthalenide **10**

Powder **8** (0.6 g) was dispersed in THF (25 ml) and lithium biphenylide (1.2 ml, 1.8 mmol) added slowly yielding a deep blue mixture. The mixture was stirred overnight affording a red slurry. Powder **10** was col-

lected and washed with THF then dried in vacuo at 35°C for 10 h as a red/brown powder (0.6 g). IR (nujol)  $\nu(\text{Al-H})$  1878 cm<sup>-1</sup>.

### 3.8. Synthesis of alane 'endcapped' silica supported lithium naphthalenide **11**

Powder **9** (0.9 g) was dispersed in THF (25 ml) and lithium biphenylide (1.2 ml, 1.8 mmol) added slowly yielding a deep blue mixture. The mixture was stirred overnight affording a red slurry. Powder **11** was collected and washed with THF then dried in vacuo at 35°C for 10 h as a red/brown powder (0.9 g).

### 3.9. Synthesis of alane and trimethylsilyl 'endcapped' silica supported sodium naphthalenide **12**

Powder **8** (1.3 g) was dispersed in THF (25 ml) and sodium biphenylide (1.5 ml, 2.3 mmol) added slowly yielding a deep blue mixture. The mixture was stirred overnight affording a bright red slurry. Powder **12** was collected and washed with THF then dried in vacuo at 35°C for 10 h as a brown powder (1.3 g). IR (nujol):  $\nu(\text{Al-H})$  1881 cm<sup>-1</sup>.

### 3.10. Synthesis of *N*-Me aminopropyl naphthalene silica **13**

A mixture of silica (1.9 g), *N*-Me(3-aminopropyl)trimethoxy silane (1.3 g), chloromethylnaphthalene (0.7 g) and triethylamine (0.5 ml) in a toluene/methanol solution was refluxed for 24 h. Volatiles were removed in vacuo and the resulting powder was washed in toluene (2 × 30 ml), water (2 × 50 ml) CHCl<sub>3</sub> (2 × 30 ml) and methanol. The product was dried in vacuo at 60°C for 6 h (2.2 g).  $^{29}\text{Si}$  NMR (79.45 MHz, CP MAS)  $\delta$  -90 to -115 (lattice silicon), -45 to -75 (OSiCH<sub>2</sub>);  $^{13}\text{C}$  NMR (100.56 MHz, CP MAS)  $\delta$  10.3 (CH<sub>2</sub>Si), 20.7 (CH<sub>2</sub>CH<sub>2</sub>CH<sub>2</sub>), 34.3 (CH<sub>3</sub>N), 52.6 (CH<sub>2</sub>N), 130.9 (C<sub>arom</sub>).

### 3.11. Synthesis of trimethylsilyl and alane 'endcapped' *N*-Me aminopropyl naphthalene silica **14**

To a suspension of **13** (2.5 g), was added 10 ml of chlorotrimethylsilane and the mixture refluxed for 6 h under nitrogen and then allowed to stir overnight at room temperature. The excess reactant was removed by distillation, and washed with water, followed by ethanol to remove traces of HCl. The silica was dried in vacuo at 60°C for 4 h, then suspended in THF (15 ml) at 0°C and H<sub>3</sub>AlNMe<sub>3</sub> (0.6 g) was slowly added. After gas evolution ceased the mixture was stirred overnight at ca. 20°C whereupon the solid was collected, washed with THF then dried in vacuo at 60°C for 2 h as a white powder (2.5 g).  $^{29}\text{Si}$  NMR (79.45 MHz, CP MAS)  $\delta$

–90 to –120 (lattice silicon), –45 to –75 (OSiCH<sub>2</sub>), 10.2 (very small/broad Si(CH<sub>3</sub>)<sub>3</sub>); <sup>13</sup>C NMR (100.56 MHz, CP MAS) δ 0.24 (very small, Si(CH<sub>3</sub>)<sub>3</sub>), 10.4 (CH<sub>2</sub>Si), 20.3 (CH<sub>2</sub>CH<sub>2</sub>CH<sub>2</sub>), 34.0 (CH<sub>3</sub>N), 52.1 (CH<sub>2</sub>N), 127.1 (C<sub>arom</sub>). [**14'** <sup>29</sup>Si NMR (79.45 MHz, CP MAS) δ –90 to –120 (lattice silicon), –45 to –70 (OSiCH<sub>2</sub>), 9.9 (very small Si(CH<sub>3</sub>)<sub>3</sub>); <sup>13</sup>C NMR (100.56 MHz, CP MAS) δ 0.6 (very small, Si(CH<sub>3</sub>)<sub>3</sub>), 10.5 (CH<sub>2</sub>Si), 21.2 (CH<sub>2</sub>CH<sub>2</sub>CH<sub>2</sub>), 34.0 (CH<sub>3</sub>N), 52.4 (CH<sub>2</sub>N), 127.9 (C<sub>arom</sub>). IR(nujol): ν(Ga–H) 1983 cm<sup>-1</sup>]

### 3.12. Synthesis of alane 'endcapped' N–Me aminopropyl naphthalene silica **15**

To a suspension of **13** (0.4 g) in THF (15 ml) at 0°C was slowly added H<sub>3</sub>Al·NMe<sub>3</sub> (0.6 g). After gas evolution ceased the mixture was stirred overnight at ca. 20°C, whereupon the solid was collected, washed with THF then dried in vacuo at 60°C for 2 h as powder **33** (0.4 g). <sup>29</sup>Si NMR (79.45 MHz, CP MAS) δ –90 to –120 (lattice silicon), –40 to –60 (OSiCH<sub>2</sub>); <sup>13</sup>C NMR (100.56 MHz, CP MAS) δ 9.5 (CH<sub>2</sub>Si), 20.7 (CH<sub>2</sub>CH<sub>2</sub>CH<sub>2</sub>), 34.3 (CH<sub>3</sub>N), 52.4 (CH<sub>2</sub>N), 132.9 (C<sub>arom</sub>). IR (nujol) ν(Al–H) 1879 cm<sup>-1</sup>. [**15'** <sup>29</sup>Si NMR (79.45 MHz, CP MAS) δ –90 to –120 (lattice silicon), –40 to –70 (OSiCH<sub>2</sub>); <sup>13</sup>C NMR (100.56 MHz, CP MAS) δ 9.8 (CH<sub>2</sub>Si), 21.0 (CH<sub>2</sub>CH<sub>2</sub>CH<sub>2</sub>), 34.3 (CH<sub>3</sub>N), 52.1 (CH<sub>2</sub>N), 130.7 (C<sub>arom</sub>). IR (nujol) ν(Ga–H) 1981 cm<sup>-1</sup>]

### 3.13. Synthesis of trimethylsilyl and alane 'endcapped' N–Me aminopropyl lithium naphthalenide silica **16**

Powder **14** (0.4 g) was dispersed in THF (25 ml) and lithium biphenylide (1.5 ml, 2.3 mmol) added slowly yielding a deep green/blue mixture. Powder **16** was collected and washed with THF then dried in vacuo at 35°C for 1 h as a brown powder (0.4 g).

### 3.14. Synthesis of alane 'endcapped' N–Me aminopropyl lithium naphthalenide silica **17**

Powder **15** (0.3 g) was dispersed in THF (25 ml) and lithium biphenylide (1.5 ml, 2.3 mmol) added slowly yielding a deep green/blue mixture. Powder **17** was collected and washed with THF then dried in vacuo at 35°C for 1 h as a brown powder (0.3 g)

### 3.15. Synthesis of trimethylsilyl and alane 'endcapped' N–Me aminopropyl sodium naphthalenide silica **18**

Powder **14** (0.4 g) was dispersed in THF (25 ml) and sodium biphenylide (1.5 ml, 2.3 mmol) added slowly yielding a deep green/blue mixture. Powder **18** was collected and washed with THF then dried in vacuo at 35°C for 1 h as a red/brown powder (0.4 g).

### 3.16. Synthesis of alane 'endcapped' N–Me aminopropyl sodium naphthalenide silica **19**

Powder **15** (0.3 g) was dispersed in THF (25 ml) and sodium biphenylide (1.5 ml, 2.3 mmol) added slowly yielding a deep green/blue mixture. Powder **18** was collected and washed with THF then dried in vacuo at 35°C for 1 h as a red/brown powder (0.3 g).

### 3.17. Synthesis of benzyl-1-(dimethylsilyl)naphthalene **28**

1-(Chlorodimethylsilyl)-naphthalene (4.15 g, 18.2 mmol) was added to a THF (50 ml) solution of benzyl magnesium chloride (0.153 M, 33.7 mmol, 220 ml) and the reaction mixture was stirred overnight at room temperature. Volatile materials were removed in vacuo and the residue taken up in hexane (70 ml), filtered to remove magnesium chloride and the solvent removed in vacuo to afford a brown oil. Distillation yielded a colourless oil **28** (3.42 g, 66%) b.p. 137°C (0.5 mmHg). (Found for **28** C, 82.46; H, 7.51%, **28** requires C, 82.53; H, 7.31. <sup>1</sup>H NMR (200 MHz, CDCl<sub>3</sub>) δ 0.0 (6H, s, Si(CH<sub>3</sub>)<sub>2</sub>), 2.2 (2H, s, SiCH<sub>2</sub>), 6.5–7.8 (12H, m, H<sub>2,3,5-8,arom</sub>); <sup>13</sup>C NMR (50.3 MHz, CDCl<sub>3</sub>) δ –1.7 (Si(CH<sub>3</sub>)<sub>2</sub>); 14.8 (SiCH<sub>2</sub>), 117.45, 124.5, 124.6, 128.7 (C<sub>arom</sub>), 125.5 (C<sub>6</sub>), 125.7 (C<sub>7</sub>), 126.1 (C<sub>3</sub>), 128.5 (C<sub>8</sub>), 129.7 (C<sub>5</sub>), 130.5 (C<sub>4</sub>), 132 (C<sub>2</sub>), 134.4 (C<sub>4a</sub>), 136.5 (C<sub>1a</sub>), 140 (C1); <sup>29</sup>Si NMR (79.45 MHz, C<sub>6</sub>H<sub>6</sub>) δ –21.8 ppm (s, Si(CH<sub>3</sub>)<sub>2</sub>).

### 3.18. Synthesis of benzyl-1-(dimethylsilyl) lithium naphthalenide **29**

Lithium (0.02 g, 2.88 mmol) was added to a solution of benzyl-1-(dimethylsilyl)naphthalene **28** (0.8 g, 2.88 mmol) in THF (100 ml). The reaction mixture was stirred overnight to give deep blue solutions. EPR *g*<sub>av</sub> = 2.0028.

### 3.19. Synthesis of benzyl-1-(dimethylsilyl) sodium naphthalenide **30**

Sodium (0.07 g, 3.04 mmol) was added to a solution of benzyl-1-(dimethylsilyl)naphthalene **28** (0.8 g, 2.88 mmol) in THF (100 ml). The reaction mixture was stirred overnight to give deep blue solutions. EPR *g*<sub>av</sub> = 2.0028.

### 3.20. Synthesis of benzyl-1-(dimethylsilyl)dihydronaphthalene **31**

To a stirred solution of lithium benzyl-1-(dimethylsilyl)naphthalenide **29** [prepared from the reaction of **28** (2 g, 7.25 mmol) and lithium powder (0.5 g, 7.25 mmol)] in THF (100 ml) was added a moist solution of

THF (25 ml) and the mixture was stirred for 1 h, resulting in the dissipation of the blue solution to a clear solution. The solution was diluted in hexane (100 ml), washed with water (2 × 25 ml) and the organic layer separated and dried over anhydrous magnesium sulphate. Removal of the solvent afforded a pale yellow oil. Analysis by <sup>1</sup>H NMR indicated a mixture of **31** and unreacted **28**, in a ratio of 95:5. <sup>1</sup>H NMR (200 MHz, CDCl<sub>3</sub>): δ 0.2 (6H, s, Si(CH<sub>3</sub>)<sub>2</sub>), 1.8 (2H, s, SiCH<sub>2</sub>), 3.4–3.7 (3H, m, 6.7–7.4, (11H, m, H<sub>2,3,5–8,arom</sub>); <sup>13</sup>C NMR (50.3 MHz, CDCl<sub>3</sub>): δ –2.5 (Si(CH<sub>3</sub>)<sub>2</sub>); 25.7 (SiCH<sub>2</sub>), 62.6 (CH<sub>2</sub>), 67.9 (CHSi), 124.0, 124.1, 128.0, 128.3 (C<sub>arom</sub>), 125.7 (C<sub>6</sub>), 126.3 (C<sub>7</sub>), 126.7 (C<sub>3</sub>), 129.1 (C<sub>2</sub>), 139.3 (C<sub>4a</sub>), 139.7 (C<sub>1a</sub>), 142.6 (C<sub>1</sub>); <sup>29</sup>Si NMR (79.45 MHz, C<sub>6</sub>H<sub>6</sub>): δ –4.8 ppm (s, Si(CH<sub>3</sub>)<sub>2</sub>).

### 3.21. Synthesis of dihydronaphthalene polymer **32,32'**

To a stirred solution of polymer supported lithium naphthalenide **6,6'** [derived from, the reaction of **3,3'**: (a) 1.5 g, 1.5 mmol; (b) 1.1 g, 2.8 mmol with lithium biphenylide (a) and (b) 2.2 ml, 3.3 mmol] in THF (50 ml) was added a moist solution of THF (25 ml) and the mixture was stirred for 1 h, resulting in the dissipation of the blue solution. The polymer was filtered, washed with THF (3 × 50 ml) dried in vacuo for 6 h at 60°C to afford a mixture of **32** and **3** (**32'** and **3'**) as a white solid, in a ratio of 90:10. <sup>29</sup>Si NMR (79.45 MHz, CP MAS) δ 5.0, –3.9; 4.7, –3.4. IR (nujol) ν(C–H) 1253, 1255 cm<sup>–1</sup>, ν(Si–C) 842, 841 cm<sup>–1</sup>.

### 3.22. Synthesis of alane 'endcapped' silica (chemisorbed)

To a suspension of silica (3.0 g) in THF (40 ml) at 0°C was slowly added H<sub>3</sub>AlNMe<sub>3</sub> (4.0 g). After gas evolution ceased the mixture was stirred overnight at ca. 20°C, whereupon the solid was collected, washed with THF then dried in vacuo at 60°C for 2 h (3.1 g). <sup>29</sup>Si NMR (79.45 MHz, CP MAS) δ –95 to –120 (lattice silicon). IR(nujol) ν(Al–H) 1880 cm<sup>–1</sup>.

### 3.23. Synthesis of alane 'endcapped' silica (physisorbed)

A mixture of silica (2.0 g) and H<sub>3</sub>AlNMe<sub>3</sub> (0.5 g) was stirred in vacuo at 60°C for 4 h (2.1 g). <sup>29</sup>Si NMR (79.45 MHz, CP MAS): δ –90 to –120 (lattice silicon). IR(nujol) ν(Al–H) 1790 cm<sup>–1</sup>.

### 3.24. Synthesis of gallane 'endcapped' silica (chemisorbed)

To a suspension of silica (2.0 g) in THF (25 ml) at 0°C was slowly added H<sub>3</sub>GaNMe<sub>3</sub> (2.2 g). After gas evolution ceased the mixture was stirred overnight at ca. 20°C, whereupon the solid was collected, washed with

THF then dried in vacuo at 60°C for 2 h (1.9 g). <sup>29</sup>Si NMR (79.45 MHz, CP MAS) δ –90 to –120 (lattice silicon). IR(nujol) ν(Ga–H) 1976 cm<sup>–1</sup>.

### 3.25. Synthesis of gallane 'endcapped' silica (physisorbed)

A mixture of silica (1.0 g) and H<sub>3</sub>GaNMe<sub>3</sub> (0.2 g) was stirred in vacuo at 60°C for 4 h (1.0 g). <sup>29</sup>Si NMR (79.45 MHz, CP MAS) δ –90 to –115 (lattice silicon). IR(nujol): ν(Ga–H) 1860 cm<sup>–1</sup>.

### 3.26. Reaction of chlorobenzene and polymer **6**

THF (75 ml) was added to polymer **6** derived from reaction of **3** (1.4 g, 1.6 mmol) with lithium biphenylide (1.1 ml, 1.7 mmol) and the reaction mixture stirred for 4 h at room temperature. A THF solution of chlorobenzene (0.15 M) was added to the resulting red slurry, yielding a colourless solution and pale yellow solid after the addition of (6 ml) of the halide solution. Quenching of aliquots with excess HCl, followed by back titration with NaOH indicated 95% lithium reagent formation. The filtrate was removed via a cannular and the polymer washed with THF (2 × 50 ml). Chlorotrimethylsilane (1 ml, 8 mmol) was added to the combined filtrate and washings, after stirring for 2 h at room temperature the resulting solution was extracted into hexane and filtered. The solvent was distilled from the mixture to afford a colourless liquid, which was shown by <sup>1</sup>H NMR and HPLC/MS analysis to be pure phenyltrimethylsilane. The recovered polymer was dried in vacuo for 12 h at 40°C to afford compound **3** and **31** in a ratio of 90:10 (1st cycle) (1.4 g, 100% total recovery).

A full set of the yields are given in Table 1. For Barbier-type reactions the products were distilled from the reaction solvent then analysed by <sup>1</sup>H and <sup>13</sup>C NMR. Distillation temperatures at ambient pressure for quenched reaction product from the reaction of lithiated complexes of **24–27** with chlorotrimethylsilane was 0°C, 170°C and 69°C, respectively, these values compare well with literature values [58].

### 3.27. Reaction of chlorobenzene and metal oxide supported lithium naphthalenides

Reactions were carried out similarly to the above, and yields were determined in the same manner. The results of this study are represented in Table 5.

### 3.28. Synthesis of 3-trimethylsilyl-1-phenyl-1-trimethylsiloxy-propane

To a solution of 3-chloro-1-phenyl-1-propanol (0.75 g, 0.44 mmol) was added LiBu<sup>n</sup> (0.3 ml, 0.47 mmol)



affording an orange solution. The resulting solution was added to a slurry of polymer **6** derived from reaction of **5** (0.9 g, 1.0 mmol) with lithium biphenylide (0.7 ml, 1.1 mmol). This resulted in the dissipation of the red colour yielding a colourless solution and pale yellow solid. The filtrate was removed via a cannular and the polymer washed with THF (12 × 50 ml). Chlorotrimethylsilane (1.3 ml, 10 mmol) was added to the combined filtrate and washings and after stirring for 2 h at room temperature. Volatiles were removed in vacuo, and the resulting orange solid was taken up in hexane, and filtered. Concentration and cooling to  $-30^{\circ}\text{C}$  afforded the bis-silylated compound as a pale orange solid (0.8 g, 80%).  $^1\text{H}$  NMR (200 MHz,  $\text{CDCl}_3$ )  $\delta$   $-0.1$  (9H, s,  $\text{Si}(\text{CH}_3)_3$ ),  $-0.5$  (9H, s,  $\text{Si}(\text{CH}_3)_3$ ),  $1.7$ – $2.0$  (3H, m,  $\text{CH}_2\text{SiMe}_3$ ,  $\text{CHOSiMe}_3$ ),  $3.68$ – $3.81$  (2H, m,  $\text{CH}_2$ ),  $6.92$ – $7.30$  (5H, m,  $\text{H}_{\text{arom}}$ );  $^{13}\text{C}$  NMR (50.3 MHz,  $\text{CDCl}_3$ )  $\delta$   $-1.5$  ( $\text{SiCH}_3$ ),  $-1.7$  ( $\text{SiCH}_3$ ),  $16.6$  ( $\text{CH}_2\text{Si}$ ),  $23.5$  ( $\text{COSiMe}_3$ ),  $40.7$  ( $\text{CH}_2$ ),  $124.0$ ,  $127.8$ ,  $128.0$ ,  $143.8$  ( $\text{C}_{\text{ph}}$ ); MS  $m/e$  118 (54%,  $\text{M}^+ - (\text{OSiMe}_3 + \text{SiMe}_3)$ ).

### 3.29. Synthesis of 9-trimethylsilyl(anthracene)

*Method A.* THF (75 ml) was added to polymer **6** derived from reaction of **3'** (1.0 g, 2.5 mmol) with lithium biphenylide (1.9 ml, 2.8 mmol) and the mixture stirred for 4 h at room temperature, then stirred at  $-78^{\circ}\text{C}$  for 1 h. A THF solution of 9-chloroanthracene (0.15 M) was added to the resulting red slurry at  $-78^{\circ}\text{C}$ , yielding a colourless solution and pale yellow solid after the addition of (13 ml, 1.95 mmol) of the halide solution. Quenching of aliquots with HCl showed 95% lithium reagent formation. The filtrate was removed via a cannular and the polymer washed with THF (2 × 50 ml). Chlorotrimethylsilane (1.3 ml, 10 mmol) was added to the combined filtrate and washings and after stirring for 2 h at room temperature the volatiles were removed in vacuo and the resulting residue extracted into hexane, concentration and cooling to  $-30^{\circ}\text{C}$  afforded pale yellow crystals of 9-(trimethylsilyl)anthracene (0.46 g, 94%).  $^1\text{H}$  and  $^{13}\text{C}$  NMR consistent with literature values [58]. *Method B.* A solution of 9-chloroanthracene (0.34 g, 1.6 mmol) in THF (40 ml) was added slowly over 30 min to a solution of **29** [derived from reaction of **28** (0.47 g, 1.7 mmol) with lithium powder (0.012 g, 1.7 mmol)] in THF (40 ml) at  $-78^{\circ}\text{C}$ . This resulted in the dissipation of the blue colour yielding a pale yellow solution, stirring was continued for a further 3 h. Chlorotrimethylsilane (0.40 ml, 3.1 mmol) was added and the resultant solution stirred for 1 h at room temperature. Volatiles were removed in vacuo, and the resulting yellow oil was taken up in hexane and filtered. Concentration and cooling to  $-30^{\circ}\text{C}$  afforded 9-(trimethylsilyl)anthracene

in a solution of **28** in hexane (0.39 g, 96%).  $^1\text{H}$  and  $^{13}\text{C}$  NMR consistent with literature values [58]. *Method C.* A solution of 9-chloroanthracene (0.34 g, 1.6 mmol) in THF (40 ml) was added slowly over 20 min to a suspension of lithium powder (0.024 g, 3.4 mmol) and **28** (0.022 g, 0.08 mmol) in THF (40 ml) at  $-78^{\circ}\text{C}$ . This resulted in the dissipation of the green colour, and the consumption of some of lithium powder yielding a pale yellow solution containing excess lithium powder. The solution was stirred for a further 2 h. Chlorotrimethylsilane (0.40 ml, 3.1 mmol) was added and the resultant solution stirred for 1 h at room temperature. Volatiles were removed in vacuo, and the resulting yellow oil was taken up in hexane and filtered. Concentration and cooling to  $-30^{\circ}\text{C}$  afforded 9-(trimethylsilyl)anthracene, with a small amount of **52** (0.40 g, 98%).  $^1\text{H}$  and  $^{13}\text{C}$  NMR data agree with literature values [58]. *Method D.* A solution of 9-chloroanthracene (0.20 g, 0.94 mmol) in THF (40 ml) was added slowly over 20 min to a suspension of lithium powder (0.024 g, 3.4 mmol) and naphthalene (0.022 g, 0.02 mmol) in THF (40 ml). This resulted in the dissipation of the green colour, and the consumption of some of lithium powder yielding a pale yellow solution containing excess lithium powder. The solution was stirred for a further 2 h. Chlorotrimethylsilane (0.40 ml, 3.1 mmol) was added and the resultant solution stirred for 1 h at room temperature. Volatiles were removed in vacuo, and the resulting yellow oil was taken up in hexane and filtered. Concentration and cooling to  $-30^{\circ}\text{C}$  afforded 9-(trimethylsilyl)anthracene, with a small amount of naphthalene (0.22 g, 95%).  $^1\text{H}$  and  $^{13}\text{C}$  NMR consistent with literature values [58].

### 3.30. Reaction of chlorobenzene and polymer **7**

THF (75 ml) was added to polymer **7** derived from reaction of **3** (1.0 g, 1.1 mmol) with sodium biphenylide (0.9 ml, 1.3 mmol) and the reaction mixture stirred for 2 h at room temperature. A THF solution of chlorobenzene (0.15 M) was added to the resulting red slurry, yielding a colourless solution and pale yellow solid after the addition of (3.2 ml, 0.48 mmol) of the halide solution. Quenching of aliquots as above indicated 88% sodium reagent formation. The filtrate was removed via a cannular and the polymer washed with THF (2 × 50 ml). Chlorotrimethylsilane (0.9 ml, 7.0 mmol) was added to the combined filtrate and washings and after stirring for 2 h at room temperature the resulting solution was extracted in the usual manner to afford a colourless liquid which was shown by  $^1\text{H}$  NMR and HPLC/MS analysis to be pure phenyltrimethylsilane (0.06 g, 82%). The recovered polymer was dried in vacuo for 12 h at  $40^{\circ}\text{C}$  to afford compound **3** and **32** in a ratio of 85:15 (1st cycle) (1.03 g, 103% total recovery).

### 3.31. Reaction of chlorobenzene and metal oxide supported sodium naphthalenides

Reactions were carried out similarly to the above, and yields determined in the same manner. The results of this study are represented in Table 3.

### Acknowledgements

We thank the Australian Research Council for support of this work, Associate Professor Lamb, University of New South Wales, for helpful discussions, and Barry Wood, The University of Queensland, for assisting in some of the XPS experiments.

### References

- [1] T.R. van den Ancker, G.R. Hanson, F. Lee, C.L. Raston, Chem. Commun., 1997, 125, and references therein
- [2] J.L. Wardell, Preparation and use in organic synthesis of organolithium and group 1A organometallics. In: F.R. Hartley (Ed.), The Chemistry of Metal-Carbon Bond, Wiley, 1987.
- [3] P.K. Freeman, L.L. Hutchinson, Tetrahedron Lett. 22 (1976) 1849.
- [4] G. Boche, D.R. Schneider, H. Wintermayr, J. Am. Chem. Soc. 102 (1980) 5697.
- [5] J.F. Garst, F.E. Barton II, J. Am. Chem. Soc. 96 (1974) 523.
- [6] V. Kalyanaraman, M.V. George, J. Organomet. Chem. 47 (1973) 225.
- [7] M. Yus, D.J. Ramon, J. Chem. Soc., Chem. Commun., 1991, 398.
- [8] M. Yus, Chem. Soc. Rev., 1996, 155, and references therein.
- [9] D.J. Ramon, M. Yus, Tetrahedron Lett. 31 (1990) 3763.
- [10] D.J. Ramon, M. Yus, Tetrahedron Lett. 31 (1990) 3767.
- [11] A. Guijarro, D.J. Ramon, M. Yus, Tetrahedron 49 (1993) 469.
- [12] A. Guijarro, M. Yus, Tetrahedron 51 (1995) 231.
- [13] A. Guijarro, M. Yus, Tetrahedron Lett. 34 (1993) 3487.
- [14] D. Guijarro, B. Mancheno, M. Yus, Tetrahedron 50 (1994) 8551.
- [15] D. Guijarro, M. Yus, Tetrahedron 50 (1994) 3447.
- [16] D. Guijarro, M. Yus, Tetrahedron Lett. 35 (1994) 2965.
- [17] D. Guijarro, G. Guillena, B. Mancheno, M. Yus, Tetrahedron 50 (1994) 3427.
- [18] J.F. Gil, D.J. Ramon, M. Yus, Tetrahedron 49 (1993) 4923.
- [19] S. Harvey, C.L. Raston, J. Chem. Soc., Chem. Commun., 1988, 652.
- [20] T.R. van den Ancker, S. Harvey, C.L. Raston, J. Organomet. Chem. 502 (1995) 35.
- [21] T.R. van den Ancker, C.L. Raston, Organometallics, 1995, 584.
- [22] D.F. Fritz, A. Sahil, H.P. Keller, E. Kovals, Anal. Chem. 98 (1976) 5706.
- [23] L.J. Bellamy, The Infra-Red Spectra of Complex Molecules, 2nd edn., Methuen, London, 1958.
- [24] A. Streitwieser, Molecular Orbital Theory for Organic Chemists, Wiley, New York, 1961.
- [25] J.F. Garst, Acc. Chem. Res. 4 (1971) 400, and reference therein.
- [26] D.W. Sindorf, G.E. Marciel, J. Am. Chem. Soc. 105 (1983) 3767.
- [27] C.A. Fyfe, Y. Zhang, P. Aroca, J. Am. Chem. Soc. 114 (1992) 3252.
- [28] J.W. De Haan, H.M. van den Bogaert, J.J. Ponjee, L.J.M. van de Ven, J. Coll. Interface Sci. 110 (1986) 591.
- [29] F. Garbassi, L. Balducci, P. Chiurlo, L. Deiana, Appl. Surf. Sci. 84 (1995) 145.
- [30] E.R. Sudholter, R. Huis, G.R. Hays, N.C.M. Alma, J. Coll. Interface Sci. 103 (1985) 554.
- [31] D.E. Leyden, D.S. Kendall, T.G. Waddell, Anal. Chim. Acta. 126 (1881) 207.
- [32] Handbook of X-ray Photoelectron Spectroscopy, Perkin Elmer, Physical Electronics Division: Eden Prairie, 1979.
- [33] A. Nylund, I. Olefjord, Surf. Interface Anal. 21 (1994) 283.
- [34] P.R. Moses, L.M. Wiler, J.C. Lennox, H.O. Finklea, J.R. Lenhard, R.W. Murray, Anal. Chem. 50 (1978) 576.
- [35] A.Yu. Stakheev, E.S. Shapiro, J. Apijok, J. Phys. Chem. 97 (1993) 5668.
- [36] S.M.A.M. Bouwens, F.B.M. van Zon, M.P. van Dijk, A.M. van der Kraan, V.H.J. de Beer, J.A.R. van Veen, D.C. Koningsberger, J. Catalysis 146 (1994) 375.
- [37] R.J. Ward, B.J. Wood, Surf. Interface Anal. 18 (1992) 679.
- [38] F.M. Elms, R.N. Lamb, P.J. Pigram, M.G. Gardiner, B.J. Wood, C.L. Raston, J. Chem. Soc., Chem. Commun., 1992, 1423.
- [39] F.M. Elms, R.N. Lamb, P.J. Pigram, M.G. Gardiner, B.J. Wood, C.L. Raston, Chem. Mater. 6 (1994) 1059.
- [40] M.G. Simmonds, L.A. Zazzera, J.F. Evans, W.L. Gladfelter, in: T.J. Montiziani, P.R. Westmoreland, F.T.J. Smith, G.R. Paz-Pujalt (Eds.), Gas Phase and Surface Chemistry in Electronic Material Processing, Mat. Res. Soc. Pittsburgh, 1995.
- [41] F.M. Elms, PhD Thesis, Griffith Univ. 1994.
- [42] K.W. Butz, F.M. Elms, C.L. Raston, R.N. Lamb, P.J. Pigram, Inorg. Chem. 32 (1993) 398.
- [43] D.F. Shriver, R.W. Parry, Inorg. Chem. 2 (1963) 1039.
- [44] S. Cucinella, A. Mazzei, W. Marconi, Inorg. Chim. Acta. Rev. 4 (1970) 51.
- [45] H.V. Noth, H. Suchy, Zeitschrift fur Anorg. Allg. Chem. 358 (1968) 44.
- [46] M.D. Healy, A.R. Barron, Angew. Chemie. Int. Ed. Engl. 31 (1992) 921.
- [47] M.D. Healy, J.W. Ziller, A.R. Barron, Organometallics 11 (1992) 3041.
- [48] M.D. Healy, M.R. Mason, P.W. Gravelle, S.G. Bott, A.R. Barron, J. Chem. Soc., Dalton Trans., 1993, 441.
- [49] G.A. Koutsantonis, F. Lee, C.L. Raston, Main Group Chem. 1 (1995) 21.
- [50] D. Wang, G.R. Hanson, Appl. Magn. Reson. 11 (1997) 401.
- [51] P.A. Anderson, P.P. Edwards, J. Chem. Soc., Chem. Commun., 1991, 915.
- [52] P.P. Edwards, J.L. Woodall, P.A. Anderson, A.R. Armstrong, M. Slaski, Chem. Soc. Rev., 1993, 305.
- [53] J.K. Ruff, F.M. Hawthorne, J. Am. Chem. Soc. 18 (1960) 679.
- [54] N.N. Greenwood, A. Storr, M.G.H. Wallbridge, Inorg. Chem. 2 (1963) 1036.
- [55] P.K. Freeman, L.L. Hutchinson, J. Org. Chem. 48 (1983) 879.
- [56] N.D. Scott, J.F. Walker, V.L. Hansley, J. Am. Chem. Soc. 58 (1936) 2442.
- [57] B.S. Furniss, A.J. Hannaford, P.W.G. Smith, A.R. Tatchell, Vogel's Textbook of Practical Organic Chemistry, 5th Edn. Longman, 1989, p. 624.
- [58] Dictionary of Organometallic Compounds, 1st edn., Vol. 2, Chapman & Hall, 1971 and 2031, pp. 1961, 1971 and 2031.